Using a preclinical mouse model of high-grade astrocytoma to optimize p53 restoration therapy

Ksenya Shchors[a,b,c,1], Anders I. Persson[d,e,f,g], Fanya Rostker[a], Tarik Tihan[a], Natalya Lyubynska[h], Nan Li[d,e], Lamorna Brown Swigart[a], Mitchel S. Berger[e,f,g], Douglas Hanahan[c], William A. Weiss[a,b,d,e,f,g], and Gerard I. Evan[a,2]

Departments of [a]Pathology, [d]Neurology, [f]Neurological Surgery, and [h]Pediatrics, [e]Sandler Neurosciences Center, and [g]Brain Tumor Research Center, University of California, San Francisco, CA 94158; [b]Helen Diller Family Comprehensive Cancer Center, University of California, San Francisco, CA 94143; and [c]Swiss Institute for Experimental Cancer Research, Swiss Federal Institute of Technology Lausanne, CH 1015 Lausanne, Switzerland

Edited by Tak W. Mak, The Campbell Family Institute for Breast Cancer Research, Ontario Cancer Institute at Princess Margaret Hospital, University Health Network, Toronto, Canada, and approved March 4, 2013 (received for review November 9, 2012)

Based on clinical presentation, glioblastoma (GBM) is stratified into primary and secondary types. The protein 53 (p53) pathway is functionally incapacitated in most GBMs by distinctive type-specific mechanisms. To model human gliomagenesis, we used a *GFAP-HRas^{V12}* mouse model crossed into the *p53ER^{TAM}* background, such that either one or both copies of endogenous p53 is replaced by a conditional *p53ER^{TAM}* allele. The p53ER^{TAM} protein can be toggled reversibly in vivo between wild-type and inactive conformations by administration or withdrawal of 4-hydroxytamoxifen (4-OHT), respectively. Surprisingly, gliomas that develop in *GFAP-HRas^{V12};p53$^{+/KI}$* mice abrogate the p53 pathway by mutating p19^{ARF}/MDM2 while retaining wild-type p53 allele. Consequently, such tumors are unaffected by restoration of their *p53ER^{TAM}* allele. By contrast, gliomas arising in *GFAP-HRas^{V12};p53$^{KI/KI}$* mice develop in the absence of functional p53. Such tumors retain a functional p19^{ARF}/MDM2-signaling pathway, and restoration of *p53ER^{TAM}* allele triggers p53-tumor–suppressor activity. Congruently, growth inhibition upon normalization of mutant p53 by a small molecule, Prima-1, in human GBM cultures also requires p14^{ARF}/MDM2 functionality. Notably, the antitumoral efficacy of p53 restoration in tumor-bearing *GFAP-HRas^{V12};p53$^{KI/KI}$* animals depends on the duration and frequency of p53 restoration. Thus, intermittent exposure to p53ER^{TAM} activity mitigated the selective pressure to inactivate the p19^{ARF}/MDM2/p53 pathway as a means of resistance, extending progression-free survival. Our results suggest that intermittent dosing regimes of drugs that restore wild-type tumor-suppressor function onto mutant, inactive p53 proteins will prove to be more efficacious than traditional chronic dosing by similarly reducing adaptive resistance.

preclinical model | Nutlin 3 | intermittent treatment

Glioblastoma (GBM) is the commonest and most lethal type of central nervous system neoplasm. Historically, GBMs are classified as primary and secondary glioblastomas, the latter developing from preexisting lower-grade astrocytic tumors. Despite their broadly similar tumor histopathologies, the genetics of human GBM is extremely diverse. Most GBMs appear to be driven by promiscuous activation of the rat sarcoma (Ras) signaling pathway, either through mutation/overexpression of receptor tyrosine kinases (1) or through inactivation of neurofibromatosis (NF1) (2).

The protein 53 (p53) tumor-suppressor pathway is functionally inactivated in almost all types of human cancer and seems to be a necessary condition for oncogenic activation. Intriguingly, however, the mechanism by which p53-mediated tumor suppression is forestalled varies in differing tumor types. For example, in colorectal, breast, and lung carcinomas, p53 itself is inactivated, either by gene loss or through structural mutation (3–5). In contrast, p53 often remains functionally competent in other cancer types, but its activation is blocked by mutations that incapacitate transduction of its upstream activating signals. Thus, overexpression or amplification of mouse double minute (*mdm2*), the gene encoding the E3-ubiquitin ligase that targets p53 for degradation by the proteasome, is frequent in prostate cancer, whereas overexpression of the p53 transcriptional inhibitor MdmX is common in retinoblastoma (6, 7). In some breast, brain, and lung tumors, the upstream inhibitor of Mdm2 activity, p14^{ARF}, is inactivated by gene loss, methylation, or repression (8–12), thus uncoupling p53 activation from oncogenic signaling (13, 14). Finally, in tumors associated with DNA tumor viruses such as HPV, simian vacuolating virus 40, and adenovirus, p53 typically is inactivated directly by viral oncoproteins.

The p53 pathway is functionally inactivated in almost all instances of GBM. However, direct inactivation of p53 itself is relatively rare in primary GBM (15); instead, the p53 pathway is compromised by deletion of the *Ink^{4a}/p14^{ARF}* locus or by amplification of *mdm2*. In contrast, mutations that directly inactivate or delete p53 itself are the norm in secondary GBM (16). More recent genome-wide systems analyses based on their transcriptome profiles have stratified gliomas into four molecular signatures: proneural, neural, classic, and mesenchymal (2). Although both oncogenic Ras signaling and inactivation of the p53 pathway are features common to GBMs of all four molecular genetic subgroups, the precise mechanism by which Ras is activated and p53 activation is curtailed varies among the four subtypes. Such differences presumably reflect the differing evolutionary ontogenies of each GBM subtype. These, in turn, intimate that therapeutic strategies may need to be tailored to each form of GBM (17). Indeed, O6-methylguanine-methyltransferase (MGMT) status (18,

Significance

Glioblastoma is the most common and aggressive form of brain cancer. GBM patients typically respond poorly to conventional therapies. The tumor-suppressor protein 53 pathway is disrupted in a majority of GBM cases. Using a mouse model that mimics the progression of human GBM, we evaluate and optimize the therapeutic efficacy of functional p53 restoration in gliomas. We show that the efficacy of p53 restoration therapy in the animal model as well as in human GBM cells is improved markedly by an episodic dosing regimen that circumvents the selective pressure for adaptive resistance when p53 function is chronically restored.

Author contributions: K.S., A.I.P., D.H., and G.I.E. designed research; K.S., A.I.P., F.R., N. Lyubynska, and N. Li performed research; M.S.B. and W.A.W. contributed new reagents/analytic tools; K.S., A.I.P., T.T., L.B.S., and G.I.E. analyzed data; and K.S., T.T., D.H., W.A.W., and G.I.E. wrote the paper.

The authors declare no conflict of interest.

This article is a PNAS Direct Submission.

Freely available online through the PNAS open access option.

[1]To whom correspondence should be addressed. E-mail: ksenya.shchors@epfl.ch.

[2]Present address: Department of Biochemistry, University of Cambridge, Cambridge CB2 1GA, United Kingdom.

This article contains supporting information online at www.pnas.org/lookup/suppl/doi:10.1073/pnas.1219142110/-/DCSupplemental.

19), isocitrate dehydrogenase (*IDH1/2*) mutation (20), EGF receptor (*EGFR*) amplification (21), and *p53* status (22) are all being assessed currently as potential determinants of personalized GBM therapy.

Several strategies for functional restoration of defective p53 pathway signaling in cancers have been proposed, including virus-mediated delivery of wild-type p53 in tumors that have lost p53 itself, inhibition of Mdm2 and/or MdmX in tumors that retain functional p53 but in which the activating signal has been disrupted, and, in tumors with inactivating structural mutations in p53, small molecules that restore wild-type p53 conformation (23–25). In GBM the standard of care—irradiation and temozolomide—is only moderately effective, and additional approaches are being evaluated (26–28), including restoration of p53 function. However, the therapeutic efficacy of specific p53-restoration therapies remains unclear. Clearly, the precise strategy for p53 restoration in any given glioblastoma will need to be tailored to the mechanism by which the pathway has been disrupted. Even then, two caveats remain. First, restored p53 function will be therapeutically effective only if GBMs harbor both sustained and obligate p53-activating signals and if they retain intact downstream p53 effector growth arrest and apoptotic functions. Second, any approach to p53 functional restoration is susceptible to defeat by secondary mutations in the restored p53 pathway. How often such secondary mutations drive relapse depends on the type of mutation responsible for secondary p53 pathway inactivation, itself a consequence of the initial mechanism of p53 pathway inactivation, on the spontaneous frequency with which such mutations arise within the tumor cell population, and on how such secondary mutations fair under the selective pressure imposed by the initial p53 restoration.

In this study, we use a preclinical model of GBM in combination with a switchable p53 allele to model the therapeutic effect of p53 pathway restoration. We show that the therapeutic efficacy of p53 pathway restoration is greatly influenced by both the initial mechanism of p53 pathway-inactivating mutation and by the temporal manner in which the selective pressure elicited by p53 pathway restoration is applied.

Results

p53 Deficiency Accelerates Initiation of Harvey Ras^{V12}-Driven Gliomagenesis. We modeled gliomagenesis in vivo using *GFAP-Harvey Ras (HRas)^{V12}* animals, 50% of which develop tumors that are histopathologically similar to human astrocytomas by age 12 wk, with a lifetime incidence of 95% (29). Although mutant *V^{12}Ha-Ras* is not prevalent in human GBMs, this well-established model exhibits MAPK pathway activation at a level comparable with human GBMs (29–32), suggesting that the levels of Ras pathway signaling in the *GFAP-HRas^{V12}* mouse model are not supraphysiological. To assess the contribution of a functional p53 pathway to the suppression of *HRas^{V12}*-induced gliomagenesis, hemizygous *GFAP-HRas^{V12}* mice were crossed into the *p53$^{KI/KI}$* [knock-in (KI)] background in which the endogenous *p53* gene has been replaced by one encoding the p53ER^{TAM} [estrogen receptor (ER)] fusion protein. p53ER^{TAM} is functional only in the presence of the synthetic steroid ligand 4-hydroxytamoxifen (4-OHT). In the absence of 4-OHT, *p53$^{KI/KI}$* mice are functionally p53^{null} (33) but are rapidly, systemically, and reversibly shifted to *p53^{wt}* upon systemic administration of tamoxifen (TAM), which is metabolized in vivo to 4-OHT. *GFAP-HRas^{V12};p53$^{KI/KI}$*, *GFAP-HRas^{V12};p53$^{+/KI}$*, and *GFAP-HRas^{V12};p53$^{+/+}$* mice were monitored daily from birth for neurological deficits indicative of astrocytoma development, including abnormal movement and tone, hunching, and hydrocephalus. Affected animals were sacrificed, brain tissue was harvested, and the presence of astrocytoma was confirmed by H&E staining and immunohistochemistry using the glial marker GFAP together with Ki67 as a marker of proliferation.

The mean latency of tumor formation in *GFAP-HRas^{V12};p53$^{+/+}$* animals was 17 wk, falling to 16 wk in *GFAP-HRas^{V12};p53$^{+/KI}$* heterozygous mice and to 9 wk in *GFAP-HRas^{V12};p53$^{KI/KI}$* animals (Fig. 1*A*). Despite these significant differences in latency, however, tumors arising from each of the different p53 backgrounds exhibited very similar pathological features, all closely resembling high-grade gliomas in human patients (Fig. 1*B*). The high-grade gliomas arising in *GFAP-HRas^{V12};p53$^{+/KI}$* and *GFAP-HRas^{V12};p53$^{KI/KI}$* mice exhibited increased cell density, nuclear polymorphism, infiltrating edges, regions of tissue necrosis, and a high Ki67-labeling index (Fig. 1*B*). Although the overall frequency of tumors among the differing p53 backgrounds was similar, p53-deficient animals exhibited accelerated formation of high-grade gliomas relative to p53 wild-type and p53 hemizygous backgrounds (Fig. 1*C*). Hence, a functional p53 pathway retards the evolution of *HRas^{V12}*-driven glial tumorigenesis.

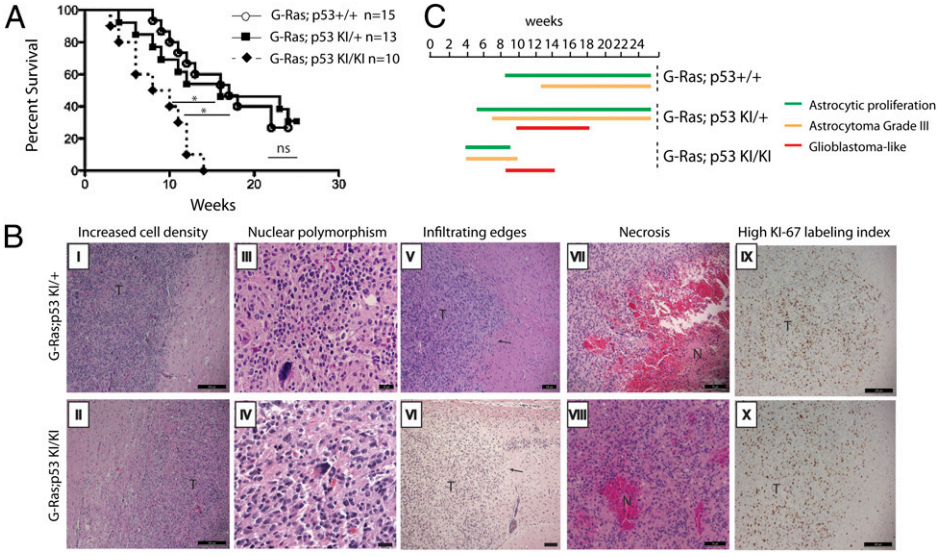

Fig. 1. Loss of p53 accelerates HRas^{V12}-induced gliomagenesis. (*A*) Survival plot (in weeks after birth) of *GFAP-HRas^{V12}* (*G-Ras*) animals from various p53 backgrounds. The size of cohorts is indicated. Statistical analysis was performed using a Mantel–Cox test. *$P < 0.01$ for *GFAP-HRas^{V12};p53$^{KI/KI}$* vs. *GFAP-HRas^{V12};p53$^{+/+}$* and *GFAP-HRas^{V12};p53$^{KI/KI}$* vs. *GFAP-HRas^{V12} ;p53$^{KI/+}$*; ns, no statistically significant (difference was detected in survival of *GFAP-HRas^{V12};p53$^{+/+}$* vs. *GFAP-HRas^{V12};p53$^{KI/+}$* animals. (*B*) Examples of H&E images of high-grade tumors arising in *GFAP-HRas^{V12};p53$^{KI/+}$* and *GFAP-HRas^{V12};p53$^{+/+}$* genetic backgrounds. Tumors exhibit increased cell density (I, II), nuclear polymorphism (III, IV), infiltrative edges (V, VI), areas of tissue necrosis (VII, VIII), and high Ki6- labeling index (IX, X). [Scale bars: 25 (III, IV), 75 (VII, VIII), 100 (V, VI), and 200 μm (I, II, IX, X)]. (*C*) A schematic representation of the onset and classification of tumors that developed in *GFAP-HRas^{V12}* animals of different p53 genotypes.

HRas^{V12}-Induced Gliomas Arising in p53-Competent Mice Retain Functional p53 but Inactivate the p53 Pathway Upstream. *GFAP-HRas^{V12};p53$^{+/KI}$* heterozygous mice harbor one wild-type and one 4-OHT–dependent copy of p53. Hence, in the absence of 4-OHT, such mice have only a single copy of p53. In other tumor models loss of the remaining functional p53 allele in both *p53$^{+/-}$* and *p53$^{+/KI}$* animals is by far the most common mechanism of p53 pathway inactivation (34–37). For example, *Eμ-myc*–driven lymphomas arising in *p53$^{+/KI}$* mice invariably inactivate the wild-type copy of p53, and subsequent restoration of the second, 4-OHT–dependent p53ER^{TAM} allele triggers dramatic p53-dependent apoptosis and tumor regression and significantly extends overall survival (37).

We reasoned that if the single wild-type p53 allele is inactivated during *GFAP-HRas^{V12};p53$^{+/KI}$* tumor progression, then restoration of the remaining conditional p53ER^{TAM} allele to wild-type function should impact tumor maintenance and subsequent progression. To address this notion, TAM, which is metabolized to the active 4-OHT ligand in vivo, was administered to symptomatic *GFAP-HRas^{V12};p53$^{+/KI}$* animals to restore p53 function, and the impact on survival was monitored. Surprisingly, restoration of function to the p53ER^{TAM} allele afforded no significant benefit in overall survival (Fig. 2*A*) and had no discernible negative impact in vivo on either the viability or proliferation of cells in *GFAP-HRas^{V12};p53$^{+/KI}$* brain tumors (Fig. 2 *B* and *C*) despite expression of the p53ER^{TAM} fusion protein in tumor tissue (Fig. S1*A*). Consistent with this finding, the restoration of p53 activity in explanted tumors in vitro by 4-OHT did not affect the proliferation nor viability of tumor cells (Fig. 2*F*) or the expression of bona fide p53 target genes (Fig. S1*B*).

Although one possible explanation for the lack of impact of TAM in *GFAP-HRas^{V12};p53$^{+/KI}$* tumors is that the 4-OHT–dependent *p53ER^{TAM}* allele had been inactivated in some way, it also is possible that the gliomas lack a requisite signal to activate p53ER^{TAM} once it has been functionally restored by TAM. In the latter scenario, functionally restored p53ER^{TAM} still should cause growth arrest and/or apoptosis in response to some other signal, for example, DNA damage (Fig. 2*D*). To determine the status of both p53 and p53ER^{TAM} in tumors arising in *GFAP-HRas^{V12};p53$^{+/KI}$* mice, tumor-bearing animals were exposed to 7 Gy of γ-radiation to activate p53 directly. As a comparison, we also irradiated tumor-bearing *p53$^{KI/KI}$* mice, which are totally deficient for p53 activity in the absence of TAM. Tumors from all irradiated animals then were analyzed for DNA damage-induced apoptosis by immunohistochemical staining for activated caspase 3 (Fig. 2*E*). Radiation-induced apoptosis was absent from tumors derived from *GFAP-HRas^{V12};p53$^{KI/KI}$* mice treated with vehicle control but was evident once p53ER^{TAM} had been functionally restored by administration of TAM, thus confirming that such apoptosis is p53 dependent (Fig. S1*C*). Radiation-induced apoptosis (3.75% of total tumor cells) was evident in the gliomas arising in *GFAP-HRas^{V12};p53$^{+/KI}$* mice irrespective of whether TAM was administered, indicating that the wild-type p53 allele was still functional (Fig. 2*E*). Similarly, radiation-induced apoptosis and the induction of p53 target genes was apparent in cultured glioma cells derived from *p53$^{+/KI}$* mice irrespective of 4-OHT (Fig. 2*G*) but not in the wild-type p53-deficient tumor cells from *p53$^{KI/KI}$* mice. In the latter case, both apoptosis and post-irradiation induction of the p53 target genes *puma* and cyclin-dependent kinase inhibitor 1a *CDKN1A* were evident only when 4-OHT was added to the medium (Fig. S1 *D* and *E*). Thus, the p53-dependent, DNA damage-induced apoptotic pathway remains intact in *GFAP-HRas^{V12};p53$^{+/KI}$* tumors. Furthermore, DNA sequence analysis confirmed that the wild-type *p53* allele in such tumors harbored no detectable mutations. Hence, gliomas arising in *GFAP-HRas^{V12};p53$^{+/KI}$* retain their functional wild-type *p53* allele.

Because p53 in *GFAP-HRas^{V12};p53$^{+/KI}$* tumors remains functional and is responsive to DNA damage, the likely explanation for its inactivity is the absence of an upstream signal to activate p53 in response to oncogenic signaling. The principal mediator of such oncogenic activation of p53 is the tumor suppressor p19^{ARF} (p14^{ARF} in humans), which is specifically induced by aberrantly elevated flux through oncogenes such as Myc and Ras (38, 39) and acts to antagonize the p53-suppressive action of Mdm2 (40, 41). This pathway may be incapacitated either through loss of p19^{ARF} itself or by overexpression of Mdm2 (Fig. 2*D*). To determine whether the p19^{ARF}/MDM2 regulatory pathway is functionally compromised in *GFAP-HRas^{V12};p53$^{+/KI}$* gliomas, we used Nutlin 3, a pharmacological inhibitor of Mdm2, to probe its functionality. Nutlin 3 induced significant apoptosis in disaggregated tumor cells from two independent *GFAP-HRas^{V12};p53$^{+/KI}$* tumors irrespective of the presence of 4-OHT (Fig. 2*H*). This effect was completely p53 dependent (Fig. S1*F*). Likewise, systemic administration of Nutlin 3 in vivo triggered significant apoptosis (13.1% of tumor cells) in tumors arising in *GFAP-HRas^{V12};p53$^{+/KI}$* mice (Fig. 2*I*), although not in wild-type p53-deficient *GFAP-HRas^{V12};p53$^{KI/KI}$* mice, without affecting the viability of normal astrocytes (Fig. 2*I*). Moreover, the level of Mdm2 protein (a target of Nutlin 3) was significantly higher in the disaggregated tumor cells from two independent *GFAP-HRas^{V12};p53$^{+/+}$* and two independent *GFAP-HRas^{V12};p53$^{+/KI}$* tumor-bearing animals than in the astrocytes isolated from their *GFAP-HRas^{V12}* transgene-negative littermates (Fig. 2*J*). These observations indicate that the block in p53 activation in *GFAP-HRas^{V12};p53$^{+/KI}$* tumors lies upstream of p53 and most probably within the Ras oncogene-sensing p19^{ARF}/MDM2 pathway.

HRas^{V12}-Induced Gliomas Arising in the Absence of Functional p53 Retain Persistent p53-Activating Signals. The studies described above all modeled the evolution of gliomas in which sporadic Ras pathway activation precedes p53 pathway inactivation, and they show that, when functional p53 itself is present, Ras activation drives selection that retains functional p53 in favor of other p53 pathway-inactivating mutations. To model the alternative evolutionary path, in which sporadic p53 loss precedes or coincides Ras activation, Ras-driven gliomas were allowed to form in *GFAP-HRas^{V12};p53$^{KI/KI}$* mice, which, in the absence of TAM, are functionally p53 null. To ascertain whether both p53-activating signals and downstream p53-mediated tumor-suppressor pathways remained competent in such tumors, we used TAM to restore p53ER^{TAM} functionally and assayed any effects of such restoration. Indeed, restoration of p53 triggered a dramatic drop in tumor cell proliferation—the proportion of actively proliferating BrdU-positive tumor cells fell from 13.3% before p53 restoration to 1.1% after p53 restoration (Fig. 3*A*)—and also induced widespread apoptosis in tumors (but not in normal tissue) (Fig. 3*B*), occasionally resulting in macroscopic destruction of the tumor mass (Fig. S2). This single transient restoration of p53, accompanied by marked induction of p53 target genes (Fig. 3*C*), significantly extended the survival of tumor-bearing *GFAP-HRas^{V12};p53$^{KI/KI}$* mice (17 d vs. 1.8 d in the non–TAM-treated controls) (Fig. 3*D*). TAM treatment of mice (p53ER-Restored) also rapidly led to a reduction in neurological deficits in animals and increased general health (Movies S1 and S2). Because p19^{ARF} is a crucial upstream regulator of p53 activity, we assayed p19^{ARF} expression in the tumors before (p53ER OFF) and 24 h after p53 restoration by addition of TAM (p53ER-Restored). The percentage of the p19^{ARF}-positive cells in tumors fell from 32.2 to 5.67% following restoration of the p53ER allele (Fig. 3*E*). We reasoned that *GFAP-HRas^{V12};p53$^{KI/KI}$* arising in the absence of functional p53 harbor persistent p53-activating signals, such as elevated levels of p19^{ARF}, which antagonize Mdm2. Upon restoration of functional p53, these p53-activating signals efficiently engage p53-mediated tumor-

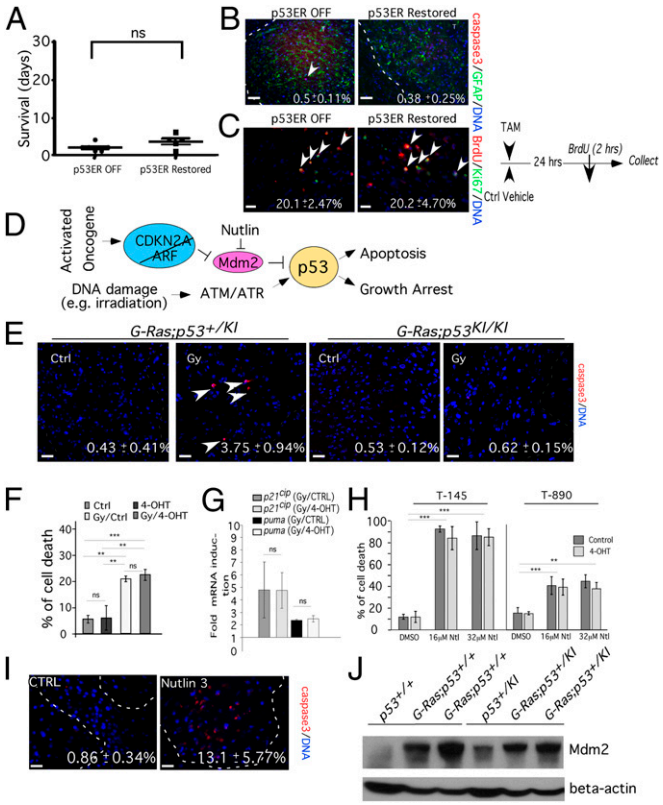

Fig. 2. Gliomas arising in p53-competent mice lose upstream p53-activating pathways. (*A*) Life span (in days after treatment) of tumor-bearing *GFAP-HRas^{V12};p53$^{+/KI}$* animals following treatment for 24 h with either vehicle (p53ER OFF; control) or TAM (p53ER Restored). Cohorts of seven animals per group were analyzed. Statistical analyses were performed using a two-tailed Student *t* test; ns, no statistical significance. (*B*) Immunohistochemical analysis of apoptosis in tumors derived from *GFAP-HRas^{V12};p53$^{+/KI}$* mice after treatment for 24 h with either vehicle (p53ER OFF; control) or TAM (p53ER Restored). Tumor area was determined by increased GFAP staining and cell density and is outlined by the dashed line. Cell death was assayed by staining for activated caspase 3. The percentage of caspase 3-positive cells out of all tumor cells is indicated. The arrow indicates the appearance of an apoptotic cell in the tumor mass. (Scale bars: 50 μm.) (*C*) (*Left*) Immunohistochemical analysis of cell proliferation status by BrdU incorporation and Ki67 staining in the tumors described in *B*. The percentage of BrdU/Ki67-positive cells out of all tumor cells is indicated. Arrows indicate double-positive cells. (Scale bars: 20 μm.) (*Right*) A schematic representation of the regimen for *p53ER^{TAM}* allele restoration is shown. A single dose of TAM was administered i.p. to symptomatic animals (p53ER Restored), and a single dose of vehicle was administered to control (Ctrl) animals (p53ER OFF). BrdU was administered 22 h later, and tissues were harvested 2 h after BrdU administration. (*D*) Schematic representation of the p53 tumor-suppressor pathway. Activated oncogene(s) (and other potential signals) induce expression from the alternate reading frame (*ARF*) of the *CDKN2A* gene, whose product, p19^{ARF}, stabilizes and activates p53 by blocking the p53 inhibitor MDM2. Activated p53 then executes its principal tumor-suppressive activities, i.e., induction of apoptosis and/or growth arrest. Loss of the *ARF* locus or up-regulation of MDM2 inactivates the functional p53 pathway. In such settings, p53 activity might be restored by the induction of an alternative p53-activating signal (e.g., DNA damage) or by pharmacological inhibition of MDM2 (e.g., by Nutlin 3). (*E*) Immunohistochemical analysis of cell death assayed by staining for activated caspase 3 in *GFAP-HRas^{V12};p53$^{+/KI}$* and *GFAP-HRas^{V12};p53$^{KI/KI}$* tumors in nonirradiated animals (Ctrl) and in animals irradiated with 7 Gy(Gy). Arrows indicate apoptotic cells. (Scale bars: 20 μm.) (*F*) Cell death depicted as the percentage of total tumor cells in in vitro tumor cell cultures derived from *GFAP-HRas^{V12};p53$^{+/KI}$* animals after treatment with vehicle (Ctrl), 4-OHT to restore p53 function (4-OHT), and irradiation (7 Gy) in combination with either vehicle treatment (Gy/Ctrl) or p53 restoration (Gy/4-OHT). The data represent experiments on three independently derived tumors analyzed in triplicate. Cell viability was determined by trypan blue exclusion. ***$P \leq 0.001$; **$P \leq 0.01$; ns, no statistical significance (statistical analyses were performed using a two-tailed Student *t* test). (*G*) Quantitative RT-PCR (qRT-PCR) analysis of mRNA expression of the p53 target genes *puma* and *p21^{cip1}* (*CDKN1A*) in cells cultured in vitro from tumors of *GFAP-HRas^{V12};p53$^{+/KI}$* animals and after exposure to 7-Gy γ-radiation in combination with 24-h exposure to 4-OHT (Gy/4-OHT) versus vehicle (Gy/CTRL). The data are presented as fold induction relative to nonirradiated samples and represent experiments from three independently derived tumors, each assayed in triplicate. ns, no statistical significance (two-tailed Student *t* test). (*H*) Percent of tumor cells undergoing apoptosis (as determined by the trypan blue exclusion method) in vitro after treatment of either vehicle-treated (dark gray bars) or 4-OHT–treated (light gray bars) tumor cell cultures derived from *GFAP-HRas^{V12};p53$^{+/KI}$* animals with the MDM2 inhibitor Nutlin 3 at a concentration of 16 (16 μM Ntl) or 32 (32 μM Ntl), or with the vehicle for Nutlin treatment (DMSO). The graph represents experimental data from two tumor cell cultures independently originated from two different tumors derived from different animals [tumor-145 (T-145) and tumor-890 (T-890)], each analyzed in triplicate. ***$P \leq 0.0001$; **$P \leq 0.001$; statistical analyses were performed using one-way ANOVA. (*I*) Immunohistochemical analysis of cell death assayed by staining for activated caspase 3 in tumors from either vehicle-treated (Ctrl)-or Nutlin 3-treated GFAP-HRas^{V12};p53$^{+/KI}$ animals. The percentage of caspase 3-positive cells out of total tumor cells is indicated. The tumor area is outlined. (Scale bars: 20 μm.) (*J*) Immunoblotting analysis of Mdm2 protein expression in tumor-derived cell cultures from *GFAP-HRas^{V12};p53$^{+/+}$* and *GFAP-HRas^{V12};p53$^{KI/+}$* animals. Two independently derived primary tumor cultures of each genotype are presented. Astrocytes isolated from the *GFAP-HRas^{V12}*-negative littermates (*p53$^{+/+}$* and *p53$^{KI/+}$*, respectively) are used as controls. β-Actin was used as an equal loading control.

suppressor pathways, resulting in the elimination of the p19^{ARF}-positive cells, presumably by apoptosis. Consistent with this hypothesis, the *GFAP-HRas^{V12};p53$^{KI/KI}$* tumors exhibited elevated levels of p19^{ARF} expression and reduced levels of Mdm2 expression compared with *GFAP-HRas^{V12};p53$^{+/KI}$* tumors that developed under selective pressure to lose p53-activating signals (Fig. S3).

To ascertain how the selective pressure exerted by p53 restoration drives secondary p53 pathway inactivation in already established *GFAP-HRas^{V12};p53$^{KI/KI}$* tumors, we restored p53 function in symptomatic 21-d-old *GFAP-HRas^{V12};p53$^{KI/KI}$* mice and then maintained p53 function for 10 subsequent weeks by daily injection of TAM (Fig. 4*A*). At this point, any symptomatic animals were presumed to harbor secondarily p53-resistant tumors. To determine whether such resistant tumors retain functional p53, symptomatic TAM-treated animals were treated with Nutlin 3 for 48 h to activate any functional p53 present, and then tumors were harvested and assayed for apoptosis. Nutlin 3 induced apoptosis (7.59% of total tumor cells) in the tumors (Fig. 4*B*), confirming that p53 (and its downstream apoptotic effectors pathway) remains functionally intact.

Because p53 is functional in these tumors, we reasoned again that its failure to block tumor growth was likely caused by the interruption of upstream p53-activating signals. Because p19^{ARF} is the mediator of oncogenic Ras signaling (39, 42), we assayed p19^{ARF} expression in both previously untreated tumors (p53ER OFF) and in tumors subjected to sustained restoration of p53 for 10 wk (p53ER-Restored Sustained) (Fig. 4 *C* and *D*). The percentage of p19^{ARF}-positive cells in the recurrent tumors growing in the face of sustained p53ER^{TAM} restoration was significantly less than in the untreated *GFAP-HRas^{V12};p53$^{KI/KI}$* tumors (Fig. 4 *C* and *D*). Intriguingly, those few tumor cells in which p19^{ARF} expression was detectable were not actively proliferating cells, as determined by their Ki67-negative status (Fig. S4), presumably a consequence of p19^{ARF}-mediated activation of the p53-induced cell-cycle arrest. Thus, our data suggest that the sustained restoration of p53 function in established *GFAP-HRas^{V12};p53$^{KI/KI}$* tumors selects for the emergence of the p53 pathway-defective tumor cells. However, such selection evidently is directed at the

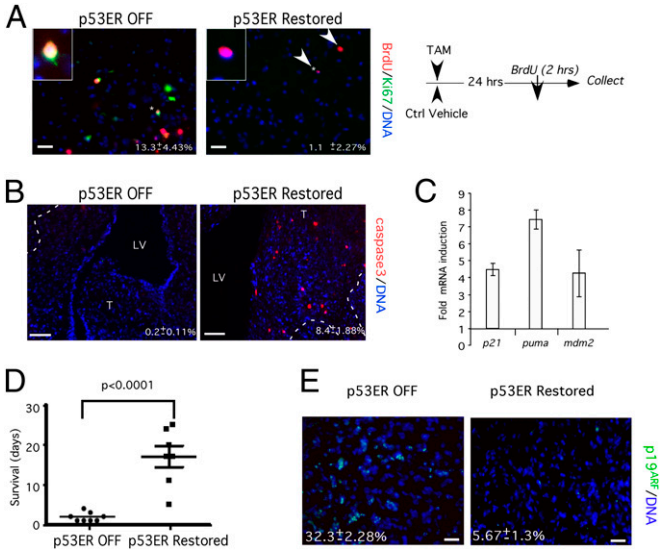

Fig. 3. Gliomas arising in the absence of functional p53 retain persistent p53-activating signals. (*A*) (*Left*) Immunohistochemical analysis of cell proliferation in *GFAP-HRas^{V12};p53$^{KI/KI}$* tumors assayed by BrdU incorporation and Ki67. A single i.p. injection of TAM (p53ER Restored) or vehicle (p53ER OFF) was administered to symptomatic *GFAP-HRas^{V12};p53$^{KI/KI}$* animals, and 22 h later the animals were injected i.p. with BrdU. Tissue samples were harvested 2 h later. Arrowheads indicate arrested, BrdU-positive/Ki67-negative cells in 4-OHT–treated tumors. (Scale bars: 50 μm.) (*Right*) A schematic representation of the regimen for *p53ER^{TAM}* allele restoration. (*B*) Immunohistochemical analysis of apoptosis in tumors after 24-h p53ER^{TAM} restoration in symptomatic *GFAP-HRas^{V12};p53$^{KI/KI}$* mice. Lateral ventricles (LV) and tumor area (T) are indicated. Cell death was assayed by staining for activated caspase 3, and the percentage of total tumor cells that are caspase 3 positive cells is indicated. (Scale bars: 100 μm.) (*C*) qRT-PCR analysis of mRNA expression of the p53 target genes *CDKN1A*, *puma*, and *mdm2* in tumor-derived cell cultures from *GFAP-HRas^{V12};p53$^{KI/KI}$* animals after 24-h exposure to 4-OHT in vitro. Data are presented as fold induction relative to vehicle-treated control samples and represent experiments on three independently derived tumors, each analyzed in triplicate. (*D*) Life spans (in days after treatment) of tumor-bearing *GFAP-HRas^{V12};p53$^{KI/KI}$* animals after 24-h treatment with either vehicle (p53ER OFF) or TAM (p53ER Restored). Cohorts of seven animals per group were analyzed. Statistical analyses were carried out using a two-tailed Student *t* test. (*E*) Immunohistochemical analysis of p19^{ARF} expression in previously untreated tumors (p53ER-OFF) compared with tumors subjected to a single TAM treatment 24 h before the sample collection (p53ER-Restored). (Scale bars: 20 μm.)

upstream p19^{ARF}/MDM2 regulators of p53 function and not against the p53 gene itself.

Optimizing of p53 Restoration Therapy. Our data indicate that restoring p53 function can exert a profound initial therapeutic impact in gliomas that evolve in the absence of functional p53. However, that therapeutic impact is eroded rapidly by the emergence of secondarily p53-resistant tumor clades that outgrow in the face of the selective pressure imposed by p53 restoration. It is known that both the rate at which adapted species arise and the evolutionary mechanism by which they do so can be influenced profoundly by whether selection is sustained or episodic (43). Given that sustained p53 restoration in *GFAP-HRas^{V12};p53$^{KI/KI}$* gliomas drives such rapid emergence of lethal secondary p53 pathway mutants, we asked how altering the timing and duration of p53 restoration influences the emergence of resistance. To start, we transiently restored p53 function once in 21-d-old *GFAP-HRas^{V12};p53$^{KI/KI}$* mice by administering a single dose of TAM. Surprisingly, even this single short period of p53 restoration significantly extended overall survival (Fig. 5*A*): 50% of controls died by 45 d compared with 74 d in 4-OHT-treated animals. Nonetheless, as with sustained TAM-treated *GFAP-HRas^{V12};p53$^{KI/KI}$* mice, all animals eventually succumbed to disease.

Relapse after transient p53 restoration might be caused by the outgrowth of tumor cells harboring mutations that confer resistance to p53ER^{TAM} restoration, in which case the recurring tumors should be resistant to subsequent p53 restoration. Alternatively, relapse might be caused by the resumed growth of a subpopulation of tumor cells that, although still sensitive to p53 restoration, undergo reversible growth arrest instead of apoptosis. In this latter case, the recurring tumors should remain responsive to subsequent p53 restoration. To distinguish between these two possibilities, 21-d-old *GFAP-HRas^{V12};p53$^{KI/KI}$* mice were subjected to a single, transient p53 restoration, which, as indicated previously, significantly delayed tumor outgrowth. The animals were monitored daily for neurological deficits indicative of astrocytoma development. Then p53 function was restored again in the symptomatic (tumor-bearing) *GFAP-HRas^{V12};p53$^{KI/KI}$* animals, and its impact on tumor apoptosis was assessed. Intriguingly, the delayed tumors remained responsive to p53 restoration, exhibiting dramatic p53-dependent apoptosis (Fig. 5*B*). However, because *GFAP-HRas^{V12}* animals might develop gliomas throughout their lifespan, the possibility existed that these delayed tumors exhibited p53 sensitivity because they had arisen de novo rather than surviving outgrowth from the original tumors. Therefore, to confirm that outgrowths from original p53-sensitive tumors subjected to transient p53 restoration indeed are sensitive to subsequent p53 restoration, we transplanted *GFAP-HRas^{V12};p53$^{KI/KI}$* tumors intracranially into congenic *p53$^{KI/KI}$* recipients and then subjected the recipient animals to a single episode of p53 restoration. Just as in the autochthonous tumors, the growth of transplanted tumors was delayed but not prevented (Fig. S5*A*). Moreover, the reemerging transplanted tumors remained largely responsive to p53-induced apoptosis following subsequent restoration of *p53ER^{TAM}* allele (Fig. S5*B*), supporting the notion that a single transient restoration of p53 in tumors does not convey resistance to the successive restoration of p53 activity. Hence, unlike tumors evolving in the presence of sustained p53 restoration, tumors recurring after a single, transient restoration of p53 function retain responsiveness to subsequent p53 restoration.

We hypothesized that p19^{ARF}, as the principal mediator of p53 activation in *GFAP-HRas^{V12};p53$^{KI/KI}$* gliomas, also was expressed in tumors arising after a single transient restoration of p53. To investigate this hypothesis, we compared expression of p19^{ARF} in tumors harvested from previously untreated, symptomatic *GFAP-HRas^{V12};p53$^{KI/KI}$* mice ("naive tumors") and from animals that succumbed to the disease after a single transient restoration of p53 at the age of 21 d (1× TAM). The tumor-bearing animals were injected with BrdU to label actively proliferating cells and were given a control vehicle or a single dose of TAM 4 h later to restore p53 transiently. Both naive tumors and tumors that reemerged after a single exposure to TAM at the age of 21 d contained p19^{ARF};BrdU double-positive cells (36.4% and 30.2% respectively) before transient restoration of p53 activity (Fig. 5*C*). The percentage of p19^{ARF};BrdU double-positive cells dropped significantly (8.6% and 6.98%, respectively) 20 h after restoration of p53 function (p53ER-Restored), suggesting that most of the actively proliferating p19^{ARF}-positive cells in both naive tumors and tumors arising in animals after transient p53 restoration (1× TAM) presumably are eliminated by apoptosis when p53 is restored for 24 h (p53ER Restored). Moreover, any remaining p19^{ARF}-positive cells still present in both the naive and 1× TAM tumors were all Ki67 negative (Fig. 5*D*), indicating their growth arrest.

Having established that tumors recurring after a single, transient restoration of p53 remain largely responsive to a second round of p53 restoration, we next asked whether repeated, in-

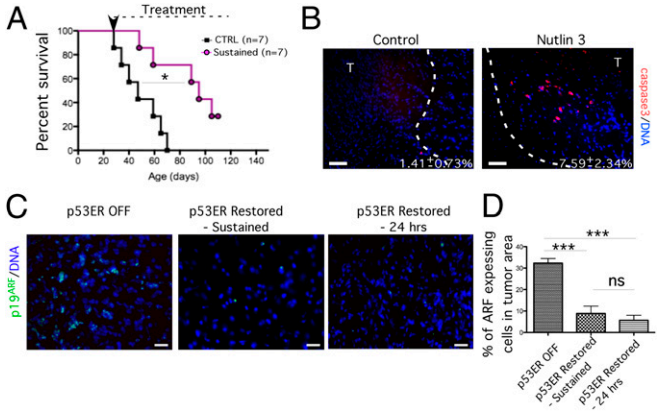

Fig. 4. Sustained restoration of p53ER^{TAM} in mouse gliomas promotes the emergence of resistant tumor variants. (*A*) Survival curves (in days after birth) of *GFAP-HRas^{V12};p53$^{KI/KI}$* animals subjected to daily treatment with vehicle (CTRL, black lines and squares) or to sustained restoration of switchable p53 (Sustained, purple lines and circles). The arrow indicates initiation of treatment. The dotted line indicates the duration of the treatment. *$P < 0.01$. The statistical analysis was performed using the Mantel–Cox test. (*B*) Immunohistochemical analysis of apoptosis as determined by activated caspase 3 in tumors collected from *GFAP-HRas^{V12};p53$^{KI/KI}$* animals 24 h after the last daily injection with 4-OHT to sustain restoration of switchable p53ER. The animals were treated with the Mdm2 inhibitor Nutlin 3 or with vehicle (Control) as described in *Materials and Methods*. The tumor area and the percentage of caspase 3-positive cells in tumors are indicated. (Scale bars: 50 μm.) (*C*) Immunohistochemical analysis of p19^{ARF} expression in previously untreated tumors (p53ER-OFF) and in tumors that developed under sustained p53ER^{TAM} restoration (p53ER-Restored-Sustained). Analysis of p19^{ARF} expression in tumors following 24-hour p53ER^{TAM} restoration (p53ER-Restored-24 hrs) is provided as a control. (Scale bars: 50 μm.) (*D*) A graphical representation of the quantification analysis of p19^{ARF}-positive cells exemplified in Fig. 4*C* is presented as the percentage of total tumor cells. At least four animals were analyzed for each treatment. Immunohistochemical analysis was performed in duplicate; 10 randomized fields per staining were considered. ***$P \leq 0.001$; ns, no statistical significance. Statistical analyses were performed using a two-tailed Student *t* test.

termittent transient p53 restoration in *GFAP-HRas^{V12};p53$^{KI/KI}$* mice might confer a therapeutic advantage over sustained p53 restoration. A cohort of 21-d-old *GFAP-HRas^{V12};p53$^{KI/KI}$* animals was subjected to transient p53 restoration (a single TAM injection) once a week for 10 wk. Remarkably, more than 80% of such intermittently treated mice remained symptom-free, surviving beyond 100 d (Fig. 5*E*).

The significant survival benefit afforded by intermittent transient p53 restoration over sustained p53 restoration suggests that, as with tumors remerging after single transient p53 restoration at age 21 d (1× TAM), the tumors retain p53 sensitivity throughout subsequent rounds of p53 restoration. To confirm this possibility, we assayed induction of apoptosis after repeated rounds of p53 restoration. Seven-week-old asymptomatic animals previously subjected either to a single dose of TAM at age 21 d (1× TAM) or to three sequential rounds of treatment with TAM once a week, starting on day 21 and with the last injection occurring at age 5 wk (Intermittent TAM), were treated with TAM (p53ER-Restored). Tissues were harvested 24 h after the last p53 restoration. After the transient restoration of p53 activity we detected similar levels of apoptosis in the lesions (8.8% and 6.8%, respectively) (Fig. 5*F*).

Because the presence of a functional p19^{ARF}/MDM2 regulatory branch is crucial for oncogenic activation of p53 tumor-suppressor response, we ascertained the status of p19^{ARF} expression in tumors subjected to intermittent restoration of p53. Brain samples for analysis were collected from 7-wk-old asymptomatic animals previously treated with a single dose of TAM at age 21 d (1× TAM) or with three sequential rounds of TAM once a week starting at age 21 d, with the last injection occurring at 5 wk of age (Intermittent TAM). Notably, and in contrast to the tumors reemerging during sustained restoration of p53 (Fig. S4), tumors reemerging in animals subjected to a single transient restoration of p53 at age 3 wk and those reemerging in animals after repeated intermittent p53 restoration retained p19^{ARF} expression in actively proliferating, Ki67-positive tumor cells (Fig. S6). Taken together, these data indicate that, unlike sustained restoration of p53, the repeated transient imposition of p53 restoration negates the otherwise strong selective advantage afforded by p53-pathway ablation in gliomas arising in *GFAP-HRas^{V12};p53$^{KI/KI}$* mice, thereby significantly enhancing the durability of the therapeutic response to p53 restoration.

Restoration of p53 Activity in Human Glioma Cultures. The *GFAP-HRas^{V12};p53$^{+/KI}$* and *GFAP-HRas^{V12};p53$^{KI/KI}$* mouse models of gliomagenesis mimic two different scenarios of human glioma progression. In both, the p53 pathway is incapacitated. In *GFAP-HRas^{V12};p53$^{+/KI}$* mice, Ras activation precedes p53 pathway inactivation, and functional p53 is retained in favor of mutations that inactivate the upstream p53-activating signal. In contrast, in the *GFAP-HRas^{V12};p53$^{KI/KI}$* mouse model, in which loss of p53function (resulting from the absence of 4-OHT) precedes or coincides with Ras activation, both upstream p53-activating signals and downstream p53-mediated arrest and apoptotic pathways remain intact. Only in this latter case would restoration of p53 function be expected to have any growth-suppressive effect. Notably, these distinctive mouse models phenocopy the two predominant modes of p53 pathway disruption in high-grade human gliomas: 42% retain functional p53 and lose ARF (*p53WT;CDKN2A (ARF) MT*), whereas ∼20% inactivate p53 directly and retain ARF (*p53MT; CDKN2A(ARF) WT*) (refs. 2 and 17 and Fig. 6*A*).

To model the therapeutic impact of p53 restoration in human gliomas of each class, we exposed human GBM cell lines (44) to 2, 2- bis(hydroxymethyl)- 3- quinuclidinone (Prima-1), a small-molecular-weight compound that restores the defective conformation of mutant p53, rescuing competence for both DNA binding and activation of p53 target genes (45). Human GBM cell lines carrying either wild-type p53 (p53WT) or mutated copies of p53 (p53MT) in combination with either competent CDKN2A (CDKN2A WT) or deleted CDKN2A (CDKN2A MT) were exposed to Prima-1 (5, 10, or 20 μM) or control vehicle for a period of 1, 3, or 5 d, and effects on cell proliferation and p53 target gene induction were ascertained. At the concentration used (20 μM), Prima-1 elicited only minor p53-independent effects (proliferation of p53WT tumors fell by 14% upon Prima-1 exposure) (Fig. 6*B*). In contrast, Prima-1 exposure induced significant growth inhibition (98% reduction in cell proliferation) in glioma cells harboring mutant p53, but only if they also retained *CDKN2A(ARF)* (Fig. 6*B*). The antiproliferative effect of Prima-1 coincided with the induction of p53 target genes [*CDKN1A* (p21^{cip1}), *mdm2*, and growth arrest and DNA damage gene 45a (*gadd45a*)] (Fig. 6*C*). This increased sensitivity of CDKN2A (ARF)-competent GBM cells to Prima-1 as compared with CDKN2A-deficient GBM cells was confirmed by analysis of an independent set of human primary GBM cultures (Fig. S7). Our data suggest that in human GBMs, as in gliomas arising in *GFAP-HRas^{V12};p53$^{KI/KI}$* mice, the presence of functional p53-activating signals is crucial to educe the p53 tumor-suppressor activities upon p53 restoration.

We next sought to determine whether in human GBM cell lines intermittent reactivation of p53 circumvents acquired resistance to p53-restoration therapy, similar to effect of intermittent p53 reactivation in the conditional mouse model. We propagated human GBM cell lines harboring mutant p53 but wild-type *CDKN2A(ARF)* in the presence of sustained or in-

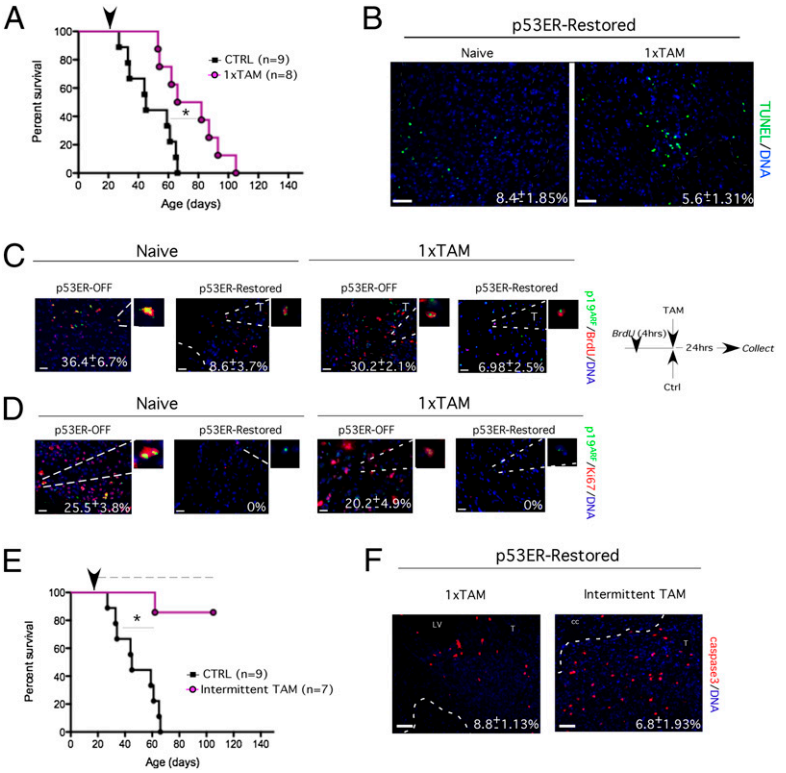

Fig. 5. Optimizing of p53-restoration therapy. (*A*) Survival curve (in days after birth) of *GFAP-HRas*^{V12};*p53*$^{KI/KI}$ animals that were untreated (CTRL. black lines and squares) or subjected to a single dose of TAM to restore p53ER^{TAM} at the age of 21 d (1× TAM, purple lines and circles). The arrowhead indicates the time point of treatment. *$P < 0.01$. Statistical analysis was performed using the Mantel–Cox test. (*B*) Immunohistochemical analysis of apoptosis in *GFAP-HRas*^{V12};*p53*$^{KI/KI}$ tumors detected by the TUNEL assay collected 24 h after exposure to TAM (p53ER-Restored). The tumors presented either developed from either previously untreated animals (naive) or were reemerging tumors following a single TAM treatment of animals at age 21 d (1× TAM). The percentage of TUNEL-positive cells in tumors is indicated. (Scale bars: 50 μm.) (*C* and *D*) (*Left*) Analysis of p19^{ARF} expression in BrdU-positive (*C*) and Ki67-positive tumor cells (*D*) in *GFAP-HRas*^{V12};*p53*$^{KI/KI}$ tumors in previously untreated animals (naive) or reemerging after a single TAM treatment at age 21 d (1× TAM). The tumor-bearing animals were injected with BrdU and 4 h later were injected with vehicle (p53ER-OFF) or with TAM (p53ER-Restored). The samples were collected 24 h later and were analyzed. The percentage of p19^{ARF}-positive cells within the populations of BrdU- and Ki67-positive cells is indicated. The dotted lines demarcate the areas enlarged in the *Insets* showing double-positive cells. (Scale bars: 20 μm.) (*Right*) A schematic representation of the treatment. (*E*) Comparative survival curves (in days after birth) of control *GFAP-HRas*^{V12} ; *p53*$^{KI/KI}$ animals (CTRL, black lines and squares) versus a cohort of mice subjected to repeated p53 restoration once a week (Intermittent TAM, purple lines and circles). The arrowhead indicates the initiation of TAM treatment. *$P < 0.01$. The dotted line indicates the duration of treatment. One animal succumbed to thymic lymphoma during the experiment and was removed from the study. Statistical analysis was performed using the Mantel–Cox test. (*F*) Immunohistochemical analysis of apoptosis by caspase 3 staining after restoration of the p53ER^{TAM} allele for 24 h (p53ER-Restored) in *GFAP-HRas*^{V12};*p53*$^{KI/KI}$ tumors reemerging in animals after a single treatment with TAM at age 3 wk (1× TAM), compared with tumors from animals subjected to three rounds of p53 restoration once a week starting at age 3 wk (Intermittent TAM). The percentage of apoptotic cells in tumor area is indicated. 1× TAM, $n = 6$; Intermittent TAM, $n = 4$ treatment. Immunohistochemical analysis was performed in duplicate; 10 randomized fields were considered. Lateral ventricles (LV), corpus callosum (cc), and tumor area (T) are indicated. (Scale bars: 50 μm.)

termittent exposure to Prima-1 at two different concentrations (10 and 20 μM) for a duration of 7 wk. At the end of the treatment, the cells were allowed to expand in Prima-1–free medium for an additional week. The resulting "sustained" and "intermittent" cultures were exposed to 0, 5, 10, and 20 μM of Prima-1 for 72 h, and effects on cell proliferation were measured. Reintroduction of Prima-1 induced a significant reduction of proliferation in GBM cultures that were propagated under intermittent exposure to Prima-1 but not in cultures subjected to sustained exposure to Prima-1 (Fig. 6*D*). This resistance of human GBM cells to chronic Prima-1 exposure was characterized by the loss of *CDKN2A(ARF)* mRNA and protein expression (Fig. 6 *E* and *F*). Our data show that in human GBM cell lines, as in the *GFAP-HRas*^{V12};*p53*$^{KI/KI}$ mouse model, transient exposure to p53 activity significantly prolongs therapeutic response to a treatment aimed to restore p53 function.

Discussion

Emerging evidence suggests that primary and secondary GBMs exhibit different patterns of genetic alterations, reflecting their distinct etiologies and potentially influencing their responsiveness to certain therapies, in particular therapies targeting specific molecular pathways (22). Alterations that diminish or abrogate the functions of the p53 tumor-suppressor pathway are seen in both primary and secondary GBM. However, p53 pathway dysfunction arises by different mechanisms in each of the two GBM subtypes. Loss of p53 itself through inactivating mutations is an early event in the multistep development of about two thirds of secondary GBM (46). In contrast, in primary GBM the p53 tumor-suppressor pathway is incapacitated most frequently by the deletion of the *Ink4/ARF* locus or by overexpression of MDM2, rather than by loss or mutational inactivation of p53 itself (15, 16, 47).

Using mice in which the *GFAP-HRas*^{V12} transgene is combined with either hemi- or homozygosity for a conditional allele of p53 (*p53*$^{KI/KI}$), we modeled the evolution of these two distinct subtypes of gliomas and ascertained the therapeutic potential of p53-based therapy in each. Although human GBMs rarely display HRas^{V12} mutations, the elevated activity of constitutively expressed HRas^{V12} produces elevated levels of MAPK pathway activation comparable to those observed in human GBMs with either EGFR or PDGF receptor A/B (PDGFR-A/B) amplification and/or activating mutations, which are common driver oncogenic mutations in human GBM (31, 48). *GFAP-HRas*^{V12};*p53*$^{KI/KI}$ mice, in which p53 is inactive throughout Ras-induced gliomagenesis, mimic the evolution of human gliomas wherein p53 itself is inactivated at the outset of tumor progression. We observed that the absence of functional p53 significantly accelerated Ras-induced gliomagenesis, consistent with the recently demonstrated role played by p53 inactivation in the progression of astrocytomas in humans (49). Functional restoration of p53 in such tumors triggered immediate p53 activation, arrest of tumor cell growth, and apoptosis, indicating that both upstream p53-activating signals and downstream tumor-suppressor effectors for apoptosis and growth arrest remained intact when p53 function was missing throughout tumorigenesis. By analogy, we predict that p53-restoration therapies are likely to be efficacious in human GBM in which p53 is inactivated early in tumor evolution.

In contrast, malignant astrocytomas developing in *GFAP-HRas*^{V12};*p53*$^{+/KI}$ mice (in which one p53 allele is wild type)

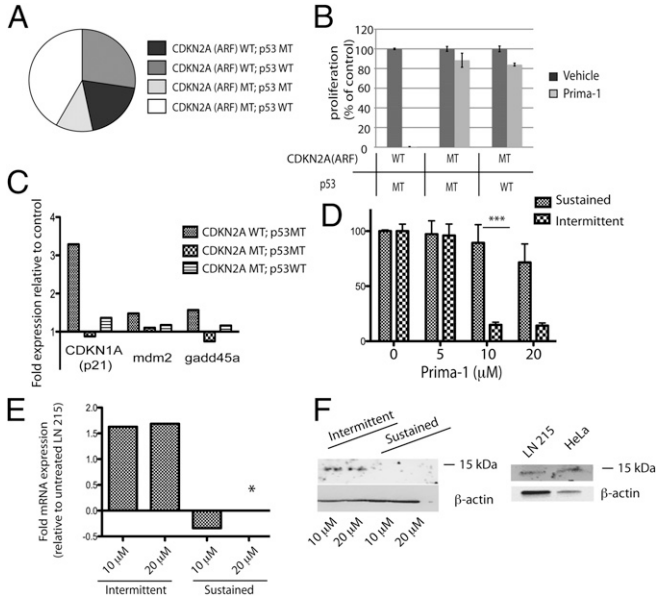

Fig. 6. Pharmacological restoration of p53 activity in human glioma cultures. (*A*) A pie chart illustrating the proportions of human glioma patients (http://tcga-data.nci.nih.gov/tcga/tcgaHome2.jsp and ref. 2) with differential status of wild-type or mutated (MT) p53 and wild-type or deleted/mutated (MT) CDKN2A(ARF). (*B*) Proliferation (presented as percent of control cultures) of human GBM cell lines (described in *Material and Methods*) with differential status of p53 and CDKN2A(ARF), mock-treated (vehicle, dark gray bars) or treated with 20 μM Prima-1 (Prima-1, light gray bars) for 5 d. (*C*) The expression of p53 target genes *CDKN1A(p21)*, *mdm2*, and *gadd45a* in the human glioma cell cultures following treatment with 5 μM Prima-1 for 24 h is presented as the fold expression relative to the control-treated samples. The expression of the target genes was normalized to ribosomal protein L13a (*RLP13A*) gene expression. The differential status of p53 and CDKN2A (ARF) are indicated. All analyses were performed in triplicate. (*D*) Proliferation (presented as percent of vehicle-treated cells) of LN 215 human GBM cells propagated on the sustained or intermittent regimens of Prima-1 treatment (10 μM) for 7 wk, as described in *Material and Methods*. Cells were treated with Prima-1 at the indicated concentrations for 72 h, and proliferation was assessed using the Cell Titer GloR luminescent assay. All experiments were repeated in triplicate. ***$P \leq 0.001$ by two-way ANOVA. Two independent cultures for each treatment (sustained and intermittent) were generated and analyzed. (*E*) The expression of $p14^{ARF}$ in LN 215 cells propagated on the sustained or intermittent regimens of Prima-1 treatment (10 or 20 μM) for 7 wk as described in *Material and Methods* is presented relative to the $p14^{ARF}$ expression in the parental LN 215 cell culture. The $p14^{ARF}$ expression was normalized to *RLP13A* gene expression. The asterisk indicates that $p14^{ARF}$ mRNA expression was below the detection level in the LN 215 cells propagated in the 20-μM sustained Prima-1 regimen. All analyses were performed in triplicate. (*F*) (*Left*) Immunoblotting analysis of $p14^{ARF}$ protein expression in LN 215 cell cultures propagated as described above. (*Right*) $p14^{ARF}$ protein expression in the parental LN 215 cells relative to HeLa cells. β-Actin was used as a loading control.

model the evolution of human tumors, such as primary GBMs, in which Ras activation precedes the loss of a functional p53 pathway (13). In such tumors restoration of p53 function is therapeutically irrelevant, because selection against the p53 pathway preferentially elicits either loss of $p19^{ARF}$ or up-regulation of Mdm2, rather than direct inactivation of p53 protein itself as observed in the *(cis)*$p53^{+/-}$;$NF1^{(+)\ flox/flox}$;*hGFAP-cre*–positive model (50). These results highlight the mutual complementarity of the two models. Indeed, human glioblastomas deficient for NF1 activity exhibit relatively low levels of total and phospho-proteins in the PI3K and MAPK pathways, indicating oncogene-signaling activity, as compared with GBMs carrying elevated expression of and/or mutations in EGFR or PDGFR A/B (48). Although restoration of functional p53 is inconsequential for p53-competent tumors, activation of p53 by Nutlin 3, an Mdm2 inhibitor, has been proven to induce cell death in these tumors (Fig. 2*I*). For gliomas with wild-type p53 status, either Nutlin 3 itself or other inhibitors of Mdm2 activity potentially can be translated into clinical settings. Unfortunately, it is impossible to predict whether in these tumors an intermittent regimen of Mdm2 inhibition in gliomas will be as efficacious as the intermittent restoration of p53 in the p53-deficient lesion. The resistance of tumor cells to treatments based on Mdm2 inhibition might be achieved by mechanisms other than resistance to p53 restoration (e.g., Mdm2 amplification).

We evaluated the potential impact of p53 restoration in human GBM cell lines that carry p53 gene mutations by using a small-molecular-weight molecule, Prima-1, that selectively restores sequence-specific DNA-binding activity to mutant forms of p53 protein. As in the $GFAP\text{-}HRas^{V12}$ -driven gliomas, the restoration of p53 activity inhibited human GBM cell proliferation. However, as in the $GFAP\text{-}HRas^{V12}$–driven gliomas, the p53 tumor-suppressor activity and the induction of p53 transcriptional targets following exposure to Prima-1 were detected only in tumors in which the p53-activating branch ($p14^{ARF}$/*MDM2)* remained intact (Fig. 6 *B* and *C* and Fig. S7). Moreover, in human GBM cells the selective pressure against the p53 pathway imposed by sustained exposure to Prima-1 results in the loss of $p14^{ARF}$ expression and subsequent resistance to the drug treatment (Fig. 6 *D*–*F*). Around 11% of all human GBMs contain mutations in both the *p53* gene and its activating tumor-suppressing branch, $p14^{ARF}$/*MDM2,* as was established recently by the molecular profile of human GBMs (http://tcga-data.nci.nih.gov/tcga/tcgaHome2.jsp and ref. 2). Our data suggest that restoration of p53 activity by Prima-1 alone [or by other small molecules modulating the DNA-binding activity of mutant p53 (51)] is not sufficient to induce p53 tumor-suppressor activity in these doubly mutant patients, and alternative means of p53 activation (e.g., DNA damage) should be considered for therapeutic intervention based on p53 restoration.

Given the prospect of using such p53-restoration therapies in GBM patients, we went on to use the $GFAP\text{-}HRas^{V12}$;$p53^{KI/KI}$ model to assess potential regimens for p53 restoration in the p53-mutant fraction of gliomas. In $GFAP\text{-}HRas^{V12}$;$p53^{KI/KI}$ tumors, sustained restoration of p53 function rapidly selects for the emergence of tumor cell populations resistant to p53 function by virtue of abrogating p53-activating signals, i.e., loss of $p19^{ARF}$ or amplification of MDM2. Further analyses established that there is a significant difference between tumors subjected to sustained p53 restoration and the tumors that developed in $GFAP\text{-}HRas^{V12}$;$p53^{KI/KI}$ animals after a short-term restoration of p53 activity. The latter emerge faster (Figs. 4*A* and 5*A*) and, surprisingly, retain $p19^{ARF}$/*MDM2* signaling (Fig. 5*B*). Thus, it appears that losing $p19^{ARF}$ does not convey growth or survival advantage to the Ras-driven tumors that have developed in the context of inactive p53 until p53 function is chronically restored. In marked contrast to the resistance mediated by the loss of $p19^{ARF}$ in chronically p53-restored tumors, the tumors remerging after a brief period of p53 restoration do not develop such resistance, as evidenced by their susceptibility to undergo apoptosis and replicative growth arrest subsequently in response to additional rounds of transient p53 restoration.

Taken together, our data imply the existence of three populations within the $GFAP\text{-}HRas^{V12}$;$p53^{KI/KI}$ tumors, each with a distinct response to p53 restoration. Two of these populations are sensitive to p53 restoration: one, comprising the bulk of tumor cells, responds to p53 restoration by apoptosis and/or permanent replicative arrest. A second, smaller, population also is responsive to p53 restoration but instead of dying undergoes viable and reversible replicative arrest. Once p53 function is removed, this second population regenerates the tumor. Clearly, the refractoriness of this second population to p53-induced apoptosis is not a heritable trait, because the bulk of cells within the

tumors from which it regenerates are, once again, susceptible to p53-induced apoptosis. Possibly such resistant glioma cells represent an innately apoptosis-resistant tumor stem cell population or, alternatively, cancer cells transiently residing in a protected somatic niche. The trivial possibility that some tumor cells survive p53 restoration through lack of exposure to 4-OHT seems unlikely, given the ubiquitous restoration of p53 that we have observed following systemic administration of 4-OHT to $p53^{KI/KI}$ mice, the facile capacity of 4-OHT to cross the blood–brain barrier, and the persistence of 4-OHT in plasma for up to 24 h following the administration of a single bolus (52, 53). In addition to these p53-sensitive populations, there evidently is a third population of tumor cells that harbors a preexisting secondary p53 pathway-inactivating mutation and that therefore is innately unresponsive to p53 restoration.

The eventual outgrowth of this third population of p53-resistant tumor cells and the p53-resistant tumor they regenerate limits how long survival may be extended by periodic p53 restoration. Hence, factors that govern the rate of outgrowth of this population will be critical in determining the overall therapeutic efficacy of p53 restoration. Although sustained p53 restoration affords a selective advantage only to innately p53-resistant tumor cells, transient p53 restoration (once relaxed) permits the outgrowth of both innately p53 resistant tumor cells and those tumor cells that are only adventitiously refractory to p53-induced apoptosis. Perhaps competition between these two populations or the differential activity of Ras signaling in tumor cells mitigates the outgrowth of the resistant tumor cells (Fig. S8). We suspect that these mechanisms underlie the greater therapeutic efficacy of intermittent versus sustained p53 restoration. However, although an intermittent regimen of a p53-reactivating treatment significantly lengthened the lifespan of tumor-bearing animals, we nonetheless detected tumors in all the intermittently treated animals surviving beyond 100 d, and all animals from the independent cohort left for surveillance following cessation of intermittent treatment eventually succumbed to disease. Hence, intermittent p53 restoration typically delays, rather than stops, disease progression. As is consistent with this effect, the human GBM cultures maintained under intermittent exposure to Prima-1 continue to proliferate once the drug is removed. These data suggest that the application of therapy based on p53 restoration in combination with other antiglioma strategies, for example conventional GBM therapies such as temozolomide, will be more beneficial for patients than temozolomide alone. In particular, patients with secondary GBMs exhibiting a high frequency of p53 mutations and displaying MGMT promoter silencing (46), which is crucial for the tumor sensitivity to temozolomide (18), could be regarded as ideal candidates. Nevertheless, our data predict a significant therapeutic advantage for intermittent versus sustained regimens of p53-restoration therapy, making intermittent therapy worthy of serious consideration in future clinical trial designs involving p53-reactivating agents.

Materials and Methods

Mice and Tissue Sample Generation, Manipulation, and Preparation. Mice were housed, fed, and treated in accordance with protocols approved by Institutional Animal Care and Use Committee at the University of California, San Francisco. *GFAP-V^{12}HaRasIRESLacZ* (*GFAP-HRas^{V12}*) (*RasD8*) animals were kindly provided by A. Guha (University of Toronto, Toronto) (29) and were crossbred into the conditional p53 (*p53$^{KI/KI}$*) background (33) to generate *GFAP-HRas^{V12};p53$^{+/+}$*, *GFAP-HRas^{V12};p53$^{+/KI}$* and *GFAP-HRas^{V12};p53$^{KI/KI}$* progeny. Hemizygous *GFAP-HRas^{V12}* animals were maintained on a mixed *129SvJ/C57Bl6/CD1* background. Functionality of the p53ER^{TAM} protein was restored in vivo by i.p. injection of TAM (1 mg/d) dissolved in peanut oil (Sigma). TAM is metabolized to the ER^{TAM} functional ligand 4-OHT in vivo, and our previous studies confirm the equivalent effects of TAM and 4-OHT when administered to animals (33). Mice were sacrificed either when they exhibited symptoms of neurological distress or at established time points. For irradiation studies, mice were exposed to 7 Gy γ-radiation using a Mark 1–68 ^{137}Cesium source (0.637 Gy/min). To inhibit MDM2 pharmacologically, mice were treated with Nutlin-3 (Cayman Chemical) administered orally through gavage (200 mg/kg), initially 24 h before administration of 4-OHT and subsequently twice each day during p53 restoration. Tissue samples were harvested 24 h after the administration of 4-OHT. Brain tissues were embedded in Optimum Cutting Temperature (OCT) medium (Sakura Finetek) or paraffin for immunohistochemical and histological H&E analyses.

Histology and Immunofluorescence. Analysis of tumor pathology was performed on the H&E-stained 5-μm paraffin-embedded brain tissue sections. Tumor grade was assigned using the World Health Organization grading scheme (54). Infiltrating gliomas were considered grade III if they exhibited mitotic figures in tumor cells. Identification of tumor necrosis or endothelial proliferation was sufficient to categorize tumors as GBM-like. Areas with increased proliferation but without the obvious nuclear pleomorphism or other features of clearly neoplastic astrocytes were classified as "astrocyte proliferation." Such astrocyte proliferation was confirmed by Ki67 staining.

For immunohistochemistry, 20-μm OCT-embedded brain tissue sections were fixed for 30 min in 1% paraformaldehyde solution. The following primary antibodies were used: rabbit monoclonal anti-Ki67 (SP6; Neomarkers), rabbit polyclonal anti–active-caspase 3 (AF 835; R&D), rat monoclonal anti-p19^{ARF} (C3; Novus), mouse monoclonal anti-BrdU (11 299 964 001; Roche), rat monoclonal anti-BrdU (OBT0030S; Accurate Chemicals), mouse monoclonal anti-GFAP (610565; BD), and rabbit polyclonal anti-ER (MC-20, SC-542; Santa Cruz). All antibodies were applied in blocking buffer [5% (wt/vol) BSA, 2.5% (vol/vol) goat serum] for 2–16 h. Secondary antibodies (Dako and Molecular Probes) were applied in blocking buffer for 1 h. TUNEL staining was performed using the Apoptag fluorescein-labeled kit (Chemicon) according to the manufacturer's directions. Fluorescent images were obtained using an LSM510 confocal microscope (Zeiss) or an Axiovert 100 inverted microscope (Zeiss) equipped with a Hamamatsu Orca digital camera, running Open Lab 3.5.1 software (Improvision).

Immunoblotting. Primary mouse cell culture was performed as described in *SI Materials and Methods*. Primary mouse tumor cultured cells and mouse astrocytes were frozen as a cell pellet at −80 °C, lysed in buffer (50 mM Tris, 150 mM NaCl, 20 mM EDTA, 0.5% Nonidet P-40) supplemented with protease and phosphatase inhibitors, and centrifuged at 20,000 × *g* for 15 min at 4 °C. Protein concentration was determined with the Bio-Rad protein assay. Protein lysates were run in 4–20% gradient gels (Invitrogen) and were blotted onto PVDF membranes (Immobilon-P). Membranes were probed with anti-Mdm2 (SMP14; BD Pharmigen), p14^{ARF} (4C6/4; Cell Signaling), and anti–β-actin (AC-15; Sigma).

Taqman Analysis and p53 Sequencing Analysis on the Mouse Tumors. Total RNA was isolated using TRIzol reagent (15596-018; Invitrogen) according to the manufacturer's protocol and DNase treated (18068–015; Invitrogen) before reverse transcription (iScript; Bio-Rad). Taqman analysis was performed by the University of California, San Francisco Comprehensive Cancer Center Genome Analysis core facility. All data were normalized to β-glucuronidase (*gus*) expression. The following probes were used: for mouse *p21*, Mm00432448_m1 (Applied Biosystems); for mouse *PUMA*, Mm00519268_m1 (Applied Biosystems); and for mouse mdm2, Mm00487656_m1 (Applied Biosystems). For p53 sequencing analysis, cDNA was amplified with primers p53 forward: 5′-CCA TGG AGG AGT CAC AGT CG-3′ and p53 reverse: 5′-GCA GAG GCA GTC AGT CTG AGT C-3′ as described (37).

Human Glioma Cell Lines. Human glioma cell lines LN18 and LN215 were kindly provided by M. Hegi (University Hospital of Lausanne, Lausanne, Switzerland). U87MG was obtained from American Type Culture Collection. The p53 and p14^{ARF} status in these cell lines was described previously (44). U87MG has wild-type *p53*, LN215 has a *p53* deletion 191–192, and LN18 has a *p53* mutation at C238S. U87MG is p14^{ARF} null, LN215 is p14^{ARF} wild type, and LN18 is p14^{ARF} null. All cells were cultured in DMEM with 10% (vol/vol) FCS. For analysis of tumor cell proliferation, glioma cell lines were plated at 3,000 cells per well in 96-well BD Falcon white/clear plates (353377; BD Bioscience) and were cultured for 1, 3, and 5 d with 0, 5, 10, and 20 μM Prima-1 (Cayman Chemical). Cell viability was analyzed by the Cell Titer GloR luminescent assay (G7570; Promega). Experiments were done in triplicate.

To generate sustained and intermittent Prima-1–treated cell populations of LN 215 cell cultures, LN 215 cells were cultured for 7 wk in the presence of 10 or 20 μM Prima-1. For weekly treatment, Prima-1 was added to the cells for 24 once a week h. Twenty-four hours later the cells were washed once in 1× PBS, and fresh drug-free medium was added. For daily treatment, the cells were exposed to Prima-1 continuously, and the medium containing

Prima-1 was replaced three times a week. At the end of the treatment, the cells were expanded in Prima-1–free medium for an additional week, and proliferation and mRNA expression were analyzed as described above. Two independent populations for each treatment were generated and analyzed. Analysis of mRNA expression of p53 target genes in human GBM cell lines was performed as described in *SI Materials and Methods*.

Statistical Analyses. Kaplan–Meier survival curves were generated using GraphPad Prism5. The statistical analysis of the survival curves was done according to the Mantel–Cox test. Tumor proliferation, apoptosis, and expression of $p19^{ARF}$ were quantified by MetaMorph Imaging V7.01 and ImageJ software (National Institutes of Health). The statistical analysis was carried out using a two-tailed Student *t* test. At least four animals were analyzed for each treatment. Immunohistochemical analysis for each antigen was performed at least in duplicate; 10 randomized fields per staining were considered.

ACKNOWLEDGMENTS. We thank Dr. Abhijit Guha and Dr. David H. Gutmann for providing the *GFAP-V^{12}HaRasIRESLacZ* animal model; Dr. Monika Hegi for providing the *LN* series human GBM cultures and for insightful criticism and advice; and Mr. Jeffrey A. Kasten and Dr. Shaun Fouse for critical reading of the manuscript. This work was supported by a grant from the Brain Tumor Society (to K.S. and G.I.E.), by National Institute of Health/National Cancer Institute Grants RO1 CA100193 (to G.I.E.) and RO1 CA102321 (to W.A.W.), by a grant from the Sante Foundation, Geneva (to D.H.), and by a grant from Samuel Waxman Cancer Research Foundation (to W.A.W. and G.I.E.). K.S. was a recipient of F32-CA106039 NIH fellowship. A.I.P. was supported by a University of California, San Francisco Specialized Program of Research Excellence Career Developmental Award and The Doctors Company Foundation.

1. Rand V, et al. (2005) Sequence survey of receptor tyrosine kinases reveals mutations in glioblastomas. *Proc Natl Acad Sci USA* 102(40):14344–14349.
2. McLendon R; Cancer Genome Atlas Research Network (2008) Comprehensive genomic characterization defines human glioblastoma genes and core pathways. *Nature* 455(7216):1061–1068.
3. Takahashi T, et al. (1989) p53: A frequent target for genetic abnormalities in lung cancer. *Science* 246(4929):491–494.
4. Malkin D, et al. (1990) Germ line p53 mutations in a familial syndrome of breast cancer, sarcomas, and other neoplasms. *Science* 250(4985):1233–1238.
5. Rodrigues NR, et al. (1990) p53 mutations in colorectal cancer. *Proc Natl Acad Sci USA* 87(19):7555–7559.
6. Osman I, et al. (1999) Inactivation of the p53 pathway in prostate cancer: Impact on tumor progression. *Clin Cancer Res* 5(8):2082–2088.
7. Laurie NA, et al. (2006) Inactivation of the p53 pathway in retinoblastoma. *Nature* 444(7115):61–66.
8. Vonlanthen S, et al. (1998) Expression of p16INK4a/p16alpha and p19ARF/p16beta is frequently altered in non-small cell lung cancer and correlates with p53 overexpression. *Oncogene* 17(21):2779–2785.
9. Maestro R, et al. (1999) Twist is a potential oncogene that inhibits apoptosis. *Genes Dev* 13(17):2207–2217.
10. Silva J, et al. (2001) Analysis of genetic and epigenetic processes that influence p14ARF expression in breast cancer. *Oncogene* 20(33):4586–4590.
11. Watanabe T, Nakamura M, Yonekawa Y, Kleihues P, Ohgaki H (2001) Promoter hypermethylation and homozygous deletion of the p14ARF and p16INK4a genes in oligodendrogliomas. *Acta Neuropathol* 101(3):185–189.
12. Maeda T, et al. (2005) Role of the proto-oncogene Pokemon in cellular transformation and ARF repression. *Nature* 433(7023):278–285.
13. Kleihues P, Ohgaki H (1999) Primary and secondary glioblastomas: From concept to clinical diagnosis. *Neuro-oncol* 1(1):44–51.
14. Biernat W, Kleihues P, Yonekawa Y, Ohgaki H (1997) Amplification and overexpression of MDM2 in primary (de novo) glioblastomas. *J Neuropathol Exp Neurol* 56(2):180–185.
15. Fulci G, et al. (2000) p53 gene mutation and ink4a-arf deletion appear to be two mutually exclusive events in human glioblastoma. *Oncogene* 19(33):3816–3822.
16. Watanabe K, et al. (1996) Overexpression of the EGF receptor and p53 mutations are mutually exclusive in the evolution of primary and secondary glioblastomas. *Brain Pathol* 6(3):217–223; discussion 223–214.
17. Verhaak RG, et al.; Cancer Genome Atlas Research Network (2010) Integrated genomic analysis identifies clinically relevant subtypes of glioblastoma characterized by abnormalities in PDGFRA, IDH1, EGFR, and NF1. *Cancer Cell* 17(1):98–110.
18. Hegi ME, et al. (2005) MGMT gene silencing and benefit from temozolomide in glioblastoma. *N Engl J Med* 352(10):997–1003.
19. Weller M, et al. (2010) MGMT promoter methylation in malignant gliomas: Ready for personalized medicine? *Nat Rev Neurol* 6(1):39–51.
20. Yan H, et al. (2009) IDH1 and IDH2 mutations in gliomas. *N Engl J Med* 360(8):765–773.
21. Haas-Kogan DA, et al. (2005) Epidermal growth factor receptor, protein kinase B/Akt, and glioma response to erlotinib. *J Natl Cancer Inst* 97(12):880–887.
22. Weller M, Stupp R, Hegi M, Wick W (2012) Individualized targeted therapy for glioblastoma: Fact or fiction? *Cancer J* 18(1):40–44.
23. Swisher SG, et al. (2003) Induction of p53-regulated genes and tumor regression in lung cancer patients after intratumoral delivery of adenoviral p53 (INGN 201) and radiation therapy. *Clin Cancer Res* 9(1):93–101.
24. Weinmann L, et al. (2008) A novel p53 rescue compound induces p53-dependent growth arrest and sensitises glioma cells to Apo2L/TRAIL-induced apoptosis. *Cell Death Differ* 15(4):718–729.
25. Selivanova G (2010) Therapeutic targeting of p53 by small molecules. *Semin Cancer Biol* 20(1):46–56.
26. Stupp R, et al.; European Organisation for Research and Treatment of Cancer Brain Tumor and Radiotherapy Groups; National Cancer Institute of Canada Clinical Trials Group (2005) Radiotherapy plus concomitant and adjuvant temozolomide for glioblastoma. *N Engl J Med* 352(10):987–996.
27. Dinca EB, et al. (2008) p53 Small-molecule inhibitor enhances temozolomide cytotoxic activity against intracranial glioblastoma xenografts. *Cancer Res* 68(24):10034–10039.
28. Lang FF, et al. (2003) Phase I trial of adenovirus-mediated p53 gene therapy for recurrent glioma: Biological and clinical results. *J Clin Oncol* 21(13):2508–2518.
29. Ding H, et al. (2001) Astrocyte-specific expression of activated p21-ras results in malignant astrocytoma formation in a transgenic mouse model of human gliomas. *Cancer Res* 61(9):3826–3836.
30. Kamnasaran D, Qian B, Hawkins C, Stanford WL, Guha A (2007) GATA6 is an astrocytoma tumor suppressor gene identified by gene trapping of mouse glioma model. *Proc Natl Acad Sci USA* 104(19):8053–8058.
31. Munoz D (2009) Transgenic mouse models of CNS tumors, using genetically engineered murine models to study the role of p21-Ras in glioblastoma multiforme. *CNS Cancer Drug Discovery and Development*, ed Van Meir EG (Humana Press, New York), pp 61–76.
32. Agnihotri S, et al. (2011) A GATA4-regulated tumor suppressor network represses formation of malignant human astrocytomas. *J Exp Med* 208(4):689–702.
33. Christophorou MA, et al. (2005) Temporal dissection of p53 function in vitro and in vivo. *Nat Genet* 37(7):718–726.
34. Donehower LA, et al. (1995) Deficiency of p53 accelerates mammary tumorigenesis in Wnt-1 transgenic mice and promotes chromosomal instability. *Genes Dev* 9(7):882–895.
35. French JE, et al. (2001) Loss of heterozygosity frequency at the Trp53 locus in p53-deficient (+/-) mouse tumors is carcinogen-and tissue-dependent. *Carcinogenesis* 22(1):99–106.
36. Vogel KS, et al. (1999) Mouse tumor model for neurofibromatosis type 1. *Science* 286(5447):2176–2179.
37. Martins CP, Brown-Swigart L, Evan GI (2006) Modeling the therapeutic efficacy of p53 restoration in tumors. *Cell* 127(7):1323–1334.
38. Junttila MR, et al. (2010) Selective activation of p53-mediated tumour suppression in high-grade tumours. *Nature* 468(7323):567–571.
39. Murphy DJ, et al. (2008) Distinct thresholds govern Myc's biological output in vivo. *Cancer Cell* 14(6):447–457.
40. Zhang Y, Xiong Y, Yarbrough WG (1998) ARF promotes MDM2 degradation and stabilizes p53: ARF-INK4a locus deletion impairs both the Rb and p53 tumor suppression pathways. *Cell* 92(6):725–734.
41. Honda R, Yasuda H (1999) Association of p19(ARF) with Mdm2 inhibits ubiquitin ligase activity of Mdm2 for tumor suppressor p53. *EMBO J* 18(1):22–27.
42. Sarkisian CJ, et al. (2007) Dose-dependent oncogene-induced senescence in vivo and its evasion during mammary tumorigenesis. *Nat Cell Biol* 9(5):493–505.
43. Huey R, Rosenzweig F (2009) Laboratory evolution meets Catch-22. *Experimental Evolution Concepts, Methods, and Applications of Selection Experi*ments, eds Garland T, Jr, and Rose MR (University of California Press, Berkeley, CA), pp 671–701.
44. Ishii N, et al. (1999) Frequent co-alterations of TP53, p16/CDKN2A, p14ARF, PTEN tumor suppressor genes in human glioma cell lines. *Brain Pathol* 9(3):469–479.
45. Lambert JM, et al. (2009) PRIMA-1 reactivates mutant p53 by covalent binding to the core domain. *Cancer Cell* 15(5):376–388.
46. Ohgaki H, Kleihues P (2007) Genetic pathways to primary and secondary glioblastoma. *Am J Pathol* 170(5):1445–1453.
47. Hayashi Y, et al. (1997) Association of EGFR gene amplification and CDKN2 (p16/MTS1) gene deletion in glioblastoma multiforme. *Brain Pathol* 7(3):871–875.
48. Brennan C, et al. (2009) Glioblastoma subclasses can be defined by activity among signal transduction pathways and associated genomic alterations. *PLoS ONE* 4(11):e7752.
49. Chow LM, et al. (2011) Cooperativity within and among Pten, p53, and Rb pathways induces high-grade astrocytoma in adult brain. *Cancer Cell* 19(3):305–316.
50. Zhu Y, et al. (2005) Early inactivation of p53 tumor suppressor gene cooperating with NF1 loss induces malignant astrocytoma. *Cancer Cell* 8(2):119–130.
51. Mandinova A, Lee SW (2011) The p53 pathway as a target in cancer therapeutics: Obstacles and promise. *Sci Transl Med* 3(64):rv1.
52. Bowman SP, Leake A, Morris ID (1982) Hypothalamic, pituitary and uterine cytoplasmic and nuclear oestrogen receptors and their relationship to the serum concentration of tamoxifen and its metabolite, 4-hydroxytamoxifen, in the ovariectomized rat. *J Endocrinol* 94(2):167–175.
53. Ringshausen I, O'Shea CC, Finch AJ, Swigart LB, Evan GI (2006) Mdm2 is critically and continuously required to suppress lethal p53 activity in vivo. *Cancer Cell* 10(6):501–514.
54. Kleihues P, Burger PC, Scheithauer BW (1993) The new WHO classification of brain tumours. *Brain Pathol* 3(3):255–268.

Supporting Information

Shchors et al. 10.1073/pnas.1219142110

SI Materials and Methods

Primary Mouse Cell Culture. Tumor tissues (identified based on high cell density, morphology, and abundance of blood vessels) were isolated using a stereo dissection microscope in ice cold 1× HBSS. Tissues were washed and treated with papain (Worthington Chemicals) for 30 min at 37 °C. Cells then were stained through a 70-μm grid and were seeded onto laminin-coated six-well plates for expansion. Primary coronal astrocytes were purified from control p6-p10 *GFAP-HRas*^{V12} transgene-negative mice by dissociation with papain, as described above, and were cultured in Neurobasal medium (Invitrogen) supplemented with 2 mM L-glutamine, B27 supplement, 20 ng/mL FGF-2, and 20 ng/mL EGF.

p53ER^{TAM} was functionally restored in vitro by the addition of 100 nM 4-OHT to the culture for the indicated period. Cell number and viability were assessed by the trypan blue exclusion method. For the irradiation experiment, cells were treated with 100 nM 4-OHT or vehicle (ethanol) for 2 h and were exposed to 7 Gy γ-radiation using a Mark 1–68 ^{137}Cesium source (0.637 Gy/min). For in vitro MDM2 inhibition studies, cells were treated with the indicated concentration of Nutlin-3 (Cayman Chemical) or control vehicle (DMSO) for 2 h before restoration of p53 with 100 nM 4-OHT. The percentage of apoptotic cells was determined by the trypan blue exclusion method. All experiments were performed on three independently derived tumor cell cultures and were performed in triplicate.

Primary Human Glioblastoma Cultures. Serially xenografted glioblastoma (GBM) 28, 14, and 43 cultures, originally isolated from patients at Mayo Clinic, Minnesota, were kindly provided by David James (University of California, San Francisco). Protein 53 (*p53*) status had been characterized previously in these cultures (1). The p53 gene in GBM28 is mutated at M246T, GBM14 has wild-type *p53*, and GBM43 has a *p53* mutation at F270C. p14^{ARF} status also had been characterized previously in these cell lines: GBM28 is p14^{ARF} wild type, whereas both GBM14 and GBM43 are p14^{ARF}-null (2). Human GBM cells were dissociated using papain and were plated on ultra-low-adherent (Corning) or polyornithine/laminin-coated plates and were cultured in Neurobasal medium (NBE) consisting of Neurobasal Medium-A, 0.5× B27 supplement, 0.5× N2 supplement (all reagents from Invitrogen), 2 mM L-glutamine, penicillin/streptavidin, 20 ng/mL basic FGF (Peprotech), and 20 ng/mL EGF (Sigma-Aldrich). Media were changed every 3 d, and cells were passaged using Accutase (Innovative Cell Technologies). Analysis of tumor cell proliferation was performed as follows: dissociated human GBM cells were plated at 3,000 cells per well in 96-well polyornithine/laminin-coated plates in NBE medium and were cultured for 5 d with 0 or 5 μM Prima-1 (Cayman Chemical). Cell numbers were estimated using total DNA content as a guide by the Cyquant NF proliferation assay (Invitrogen) according to the manufacturer's protocol. A standard curve was generated by plotting the number of plated cells (1,000–40,000) against corresponding fluorescent values, resulting in the equation $y = x + 150$, $R^2 = 1$. The number of cells in each sample was calculated using this equation. Experiments were done in triplicate.

To analyze mRNA expression of p53 target genes in human GBM cell lines, total RNA was isolated from the cell lines described in *Materials and Methods* and treated with 0 or 5 μM of Prima-1 for 24 h. To analyze mRNA expression of p53 target genes in the primary human glioblastoma cultures described above, the cultures were treated with 0 or 5 μM of Prima-1 for 5 d. The cDNA was synthesized with the iScript cDNA synthesis kit (Bio-Rad) according to the manufacturer's protocol. The expression analysis was performed with the RotorGene SybrGreen PCR kit (Qiagen) on the RotorGeneQ and was analyzed with RotorGeneQ series Software (Qiagen). The following primers were used for the analysis: *CDKN1A(p21)* forward: 5′-TGT CCG TCA GAA CCC ATG C-3′, reverse: 5′-AAA GTC GAA GTT CCA TCG CTC-3′; *mdm2* forward: 5′-TCG TCG GGT GAG GGT ACT G-3′, reverse: 5′-AAC CAC TTC TTG GAA CCA GGT-3′; *gadd45a* forward: 5′-GAG AGC AGA AGA CCG AAA GGA-3′, reverse: 5′-CAG TGA TCG TGC GCT GAC T-3′. All data were normalized to ribosomal protein L13a (*RPL13A*) and *β-actin* expression. *RPL13A* forward: 5′-GCC ATC GTG GCT AAA CAG GTA-3′, reverse: 5′-GTT GGT GTT CAT CCG CTT GC-3′; *β-actin* forward: 5′-CAT GTA CGT TGC TAT CCA GGC-3′, reverse: 5′-CTC CTT AAT GTC ACG CAC GAT-3′. All analyses were done in triplicate.

Tumor Cell Transplantation Experiment. Tumor cells were harvested from *GFAP-Harvey Ras (HRas)*^{V12}*;p53*$^{KI/KI}$ [knock-in (KI)] animals and were cultured briefly in NBE medium [Neurobasal-A (Invitrogen), penicillin/streptavidin, 2 mM L-glutamine, B27 supplement (Invitrogen), 20 ng/mL FGF-2 (Peprotech), and 20 ng/mL EGF (Sigma-Aldrich)]. The tumor cells (8×10^4 in 10 μL NBE medium) then were engrafted intracranially into anesthetized transgene-negative *p53*$^{KI/KI}$ littermates (1.5 mm lateral and 2 mm posterior to the bregma and 3 mm deep) using a Hamilton syringe and a stereotactic rig. Animals were monitored daily for symptoms of glioma. A single injection of either tamoxifen (TAM) or vehicle was administered i.p. to recipient animals 3 wk after transplantation. Each cohort consisted of seven animals, and the experiment was repeated twice with independently purified tumors.

1. Carlson BL, et al. (2009) Radiosensitizing effects of temozolomide observed in vivo only in a subset of O6-methylguanine-DNA methyltransferase methylated glioblastoma multiforme xenografts. *Int J Radiat Oncol Biol Phys* 75(1):212–219.

2. Sarkaria JN, et al. (2006) Use of an orthotopic xenograft model for assessing the effect of epidermal growth factor receptor amplification on glioblastoma radiation response. *Clin Cancer Res* 12(7 Pt 1):2264–2271.

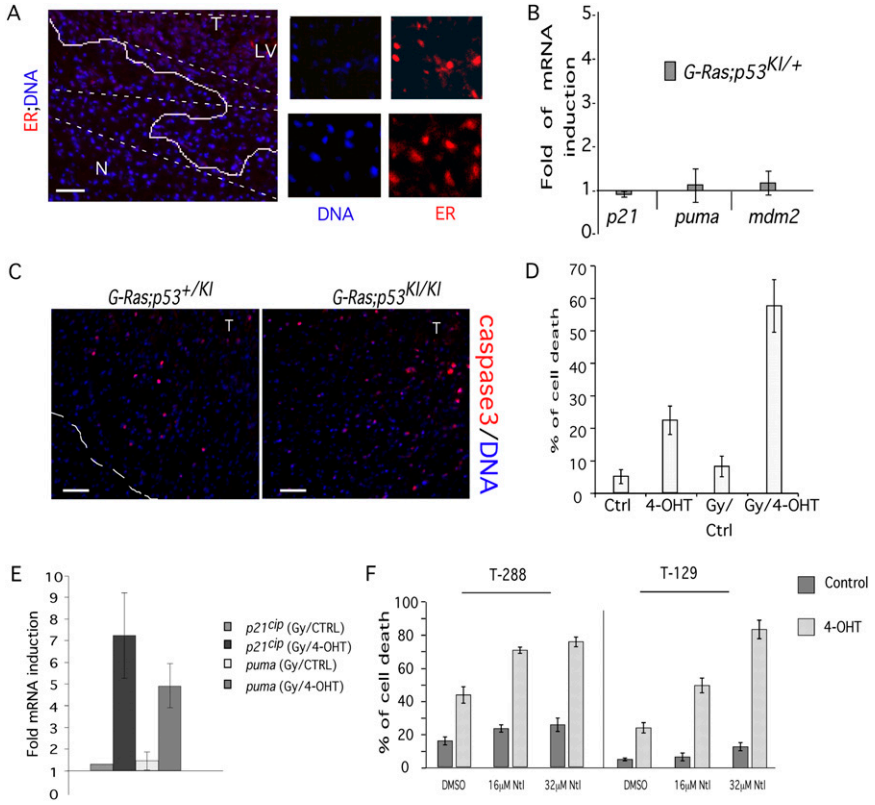

Fig. S1. Gliomas arising in *GFAP-HRas*^{V12}*;p53*$^{+/KI}$ mice but not in *GFAP-HRas*^{V12}*;p53*$^{KI/KI}$ mice lose upstream p53-activating pathways. (*A*) Immunohistochemical analysis of *p53ER*^{TAM} [estrogen receptor (ER)] allele expression in the brain tissue from tumor-bearing *GFAP-HRas*^{V12}*;p53*$^{+/KI}$ animals. The normal brain tissue (N) and tumor area (T) were determined by the density of tissue cellularity. The dotted lines demarcate the areas enlarged at right showing comparable *p53ER*^{TAM} allele expression in normal and tumor areas. Lateral ventricles (LV) are indicated. (Scale bars: 50 μm.) (*B*) Quantitative RT-PCR (qRT-PCR) analysis of mRNA expression of the p53 target genes cyclin-dependent kinase inhibitor 1a (*CDKN1A*) (*p21*^{cip1}), *puma*, and mouse double minute (*mdm2*) in tumor-derived cell cultures from *GFAP-HRas*^{V12}*;p53*$^{+/KI}$ animals after 24-h exposure to 4-hydroxytamoxifen (4-OHT) in vitro. Data are presented as fold induction relative to control (vehicle-treated) samples. The data present experiments on three independently derived tumors, each analyzed in triplicate. (*C*) Immunohistochemical analysis of cell death in *GFAP-HRas*^{V12}*;p53*$^{+/KI}$ (*Left*) and *GFAP-HRas*^{V12}*;p53*$^{KI/KI}$ (*Right*) tumors from animals treated with TAM for 2 h before exposure to 7-Gy whole-body γ-radiation. Cell death is indicated by staining for activated caspase 3. The tumor boundary is indicated in the left panel. (Scale bars: 50 μm.) (*D*) Percent of total tumor cell death in vitro of cultured glioma cells derived from *GFAP-HRas*^{V12}*;p53*$^{KI/KI}$ animals after treatment with vehicle (Ctrl), restoration of p53ER^{TAM} allele for 24 h (4-OHT), and irradiation (7 Gy) in combination with vehicle treatment (Gy/CTRL) or p53 restoration (Gy/4-OHT). The data are derived from three independently derived tumors, each analyzed in triplicate. (*E*) qRT-PCR analysis of mRNA expression of p53 target genes *puma* and *CDKN1A* in cultured cancer cells derived from tumors from *GFAP-HRas*^{V12}*;p53*$^{KI/KI}$ animals. Cells were exposed in vitro to γ-radiation in combination with 24-h exposure to 4-OHT (Gy/4-OHT) or vehicle (Gy/CTRL). The data are presented as fold induction relative to nonirradiated samples. The data represent experiments on three independently derived tumors, each analyzed in triplicate. (*F*) Percent of total tumor cells undergoing apoptosis in control-treated (dark gray bars) or 4-OHT–treated (light gray bars) tumor cell cultures derived from *GFAP-HRas*^{V12}*;p53*$^{KI/KI}$ animals and after treatment in vitro with the MDM2 inhibitor Nutlin 3 at concentrations of 16 (16 μM Ntl) or at 32 μM (32 μM Ntl) or with the vehicle for Nutlin treatment, DMSO. The data represent experiments on two tumor-cell cultures independently derived from different tumor-bearing animals (T-288 and T-129, respectively), each analyzed in triplicate.

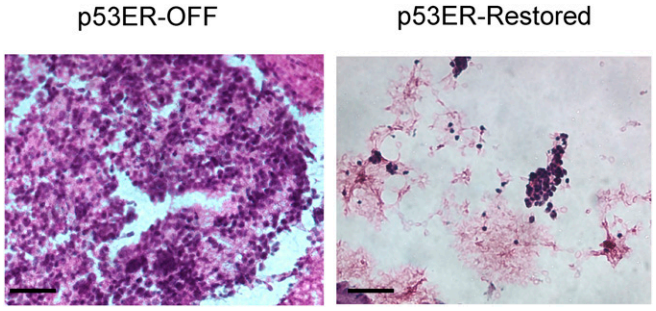

Fig. S2. Restoration of p53ER^{TAM} function in *GFAP-HRas*^{V12}*;p53*$^{KI/KI}$ tumor-bearing animals partially ablates tumors and reestablishes animal well-being. Representative H&E analysis of tumors collected from *GFAP-HRas*^{V12}*;p53*$^{KI/KI}$ animals treated with vehicle (p53ER-OFF) or TAM (p53ER-Restored) for 24 h. (Scale bars: 20 μm.)

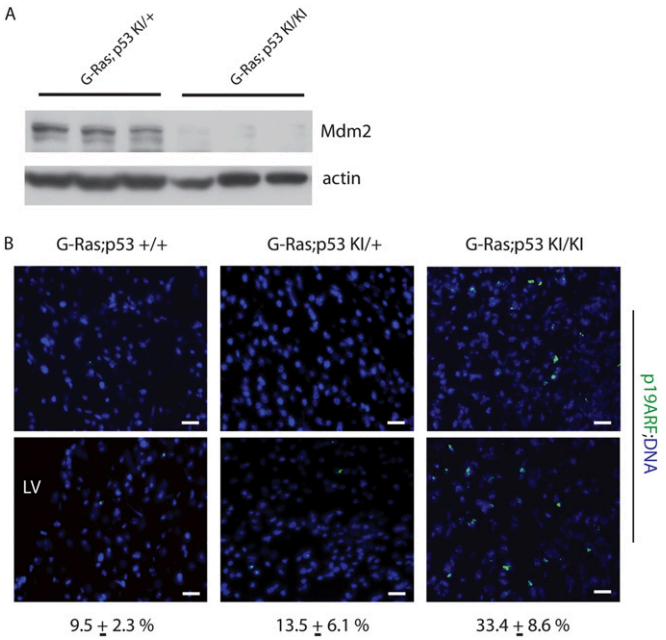

Fig. S3. Gliomas arising in the absence of functional p53 retain the p53-activating pathway. (*A*) Immunoblotting analysis of Mdm2 expression in tumor-derived cell cultures from *GFAP-HRas^{V12};p53$^{KI/+}$* and *GFAP-HRas^{V12};p53$^{KI/KI}$* animals. Three independently derived GBM cultured cells of each genotype are presented. β-Actin was used as an equal loading control. (*B*) Immunohistochemical analysis of p19^{ARF} expression in *GFAP-HRas^{V12};p53$^{+/+}$*, *GFAP-HRas^{V12};p53$^{KI/+}$*, and *GFAP-HRas^{V12};p53$^{KI/KI}$* tumors. The location of the lateral ventricle (LV) is indicated, and the percentage of p19^{ARF}-positive cells in tumors is shown below the images. (Scale bars: 20 μm.)

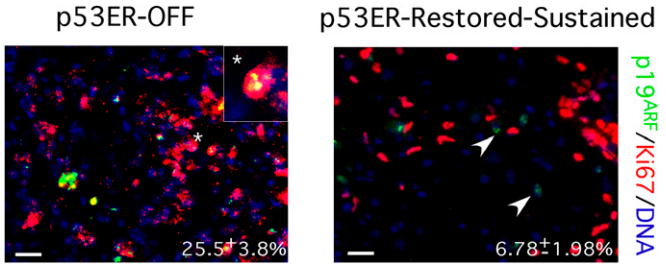

Fig. S4. Gliomas arising during sustained restoration of p53 lack p19^{ARF} expression in the actively proliferating cells. Immunohistochemical analysis of p19^{ARF} expression (green) in Ki67-positive cells (red) in control tumors (p53ER-OFF) and in tumors subjected to the sustained restoration of switchable p53 (p53ER-Restored-Sustained). The star marks the location of the area enlarged in the *Inset*. Arrowheads point to p19^{ARF}-positive cells in the p53ER-Restored-Sustained tumors. At least four animals were analyzed for each treatment. Immunohistochemical analysis was performed in duplicate; 10 randomized fields per staining were considered. The percentage of p19^{ARF}-positive cells is indicated. (Scale bars: 20 μm.)

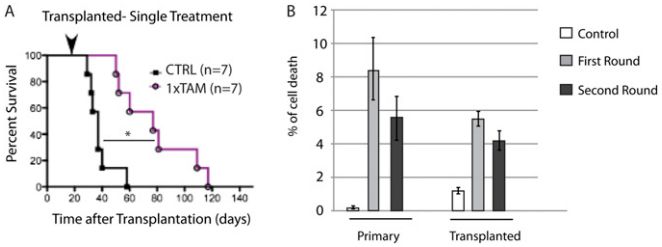

Fig. S5. *GFAP-HRas^{V12};p53$^{KI/KI}$* tumors transplanted intracranially into recipient mice retain p53-activating signals. (*A*) Survival curves (shown as days after transplantation) of *p53$^{KI/KI}$* animals transplanted with tumors derived from TAM-untreated (naive) *GFAP-HRas^{V12};p53$^{KI/KI}$ mice*. Because gliomas arise continuously in *GFAP-HRas^{V12};p53$^{KI/KI}$* mice, it is reasonable to assume that the tumors emerging after single, transient restoration of *p53ER^{TAM}* allele (presented in Fig. 5*B*) are de novo tumors rather than recurring lesions. To address this point, primary tumors isolated from TAM-naive *GFAP-HRas^{V12};p53$^{KI/KI}$* mice were transplanted into *p53$^{KI/KI}$* congenic recipients. Three weeks after the transplantation, animals were subjected to a single TAM treatment to restore p53 function transiently (1× TAM, purple lines and circles) or to vehicle (CTRL, black lines and squares). (The arrowhead indicates the time point of the treatment after transplantation.) The *p53$^{KI/KI}$* animals transplanted with *GFAP-HRas^{V12};p53$^{KI/KI}$* cancer cells succumb to recurring tumors after a single transient activation of *p53ER^{TAM}* allele. $*P < 0.01$. Statistical analyses were performed using the Mantel–Cox test. (*B*) Graph showing apoptotic tumor cells as a percentage of total tumor cells determined by the TUNEL assay. Restoration of p53 function induces apoptosis in transplanted tumors recurring after 24-h restoration of the *p53ER^{TAM}* allele. The primary tumors (Primary) that develop in *GFAP-HRas^{V12};p53$^{KI/KI}$* animals undergo apoptosis in response to a transient restoration of the *p53ER^{TAM}* allele by TAM (First Round; also see Fig. 3*A*). The tumors recurring after the first round of a transient *p53ER^{TAM}* restoration retain p53-activating signals and die by apoptosis following a subsequent 24-h restoration of p53 (Second Round; also see Fig. 5*B*). The transplanted *GFAP-HRas^{V12};p53$^{KI/KI}$* tumors (Transplanted) that develop in recipient *p53$^{KI/KI}$* animals also retain the p53-activating signals and respond by apoptotic cell death to a 24-h restoration of *p53ER^{TAM}* (First Round), and a subsequent 24-h restoration of p53 activity in recurring tumors described in Fig. S3*A* (Second Round). Five independent tumors were analyzed for each data point. Ten randomized fields were analyzed.

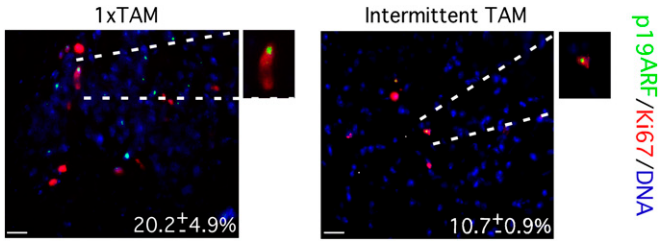

Fig. S6. *GFAP-HRas^{V12};p53$^{KI/KI}$* tumors recurring after a transient restoration of p53ER^{TAM} retain p19^{ARF} expression. Immunohistochemical analysis of p19^{ARF} and Ki67 in *GFAP-HRas^{V12};p53$^{KI/KI}$* tumors that reemerge in animals after a single treatment with TAM (1x TAM) at age 3 wk compared with tumors from animals subjected to weekly rounds of 24-h-long p53ER^{TAM} restoration starting at age 3 wk (Intermittent TAM). Dotted lines indicate areas enlarged in *Insets*. The percentage of total tumor cells positive for p19^{ARF}/Ki67 is indicated. (Scale bars: 20 μm.)

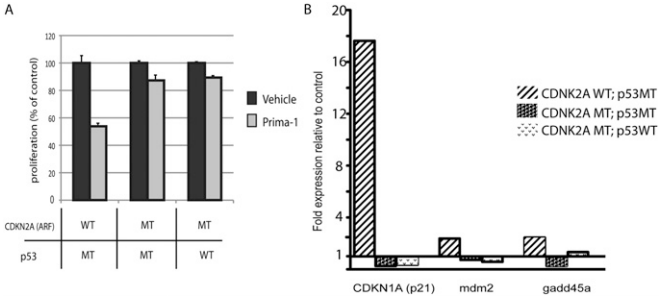

Fig. S7. Restoration of p53 activity in human glioma cell lines. (*A*) Proliferation (presented as percent of control) of primary human cell lines (described in *SI Materials and Methods*) with differential p53 and CDKN2A(ARF) status, mock-treated (dark gray bars) or treated with 20 μM Prima-1 (light gray bars) for 5 d. MT, mutated. (*B*) The expression of p53 target genes *CDKN1A(p21, mdm2*, and growth arrest and DNA damage gene 45a (*gadd45*) in the primary human glioma cell cultures after Prima-1 treatment is presented as the fold expression relative to the vehicle-treated control samples. The expression of the target genes was normalized to ribosomal protein L13a (*RLP13A*) gene expression. The differential status of p53 and CDKN2A (ARF) is indicated. All analyses were performed in triplicate.

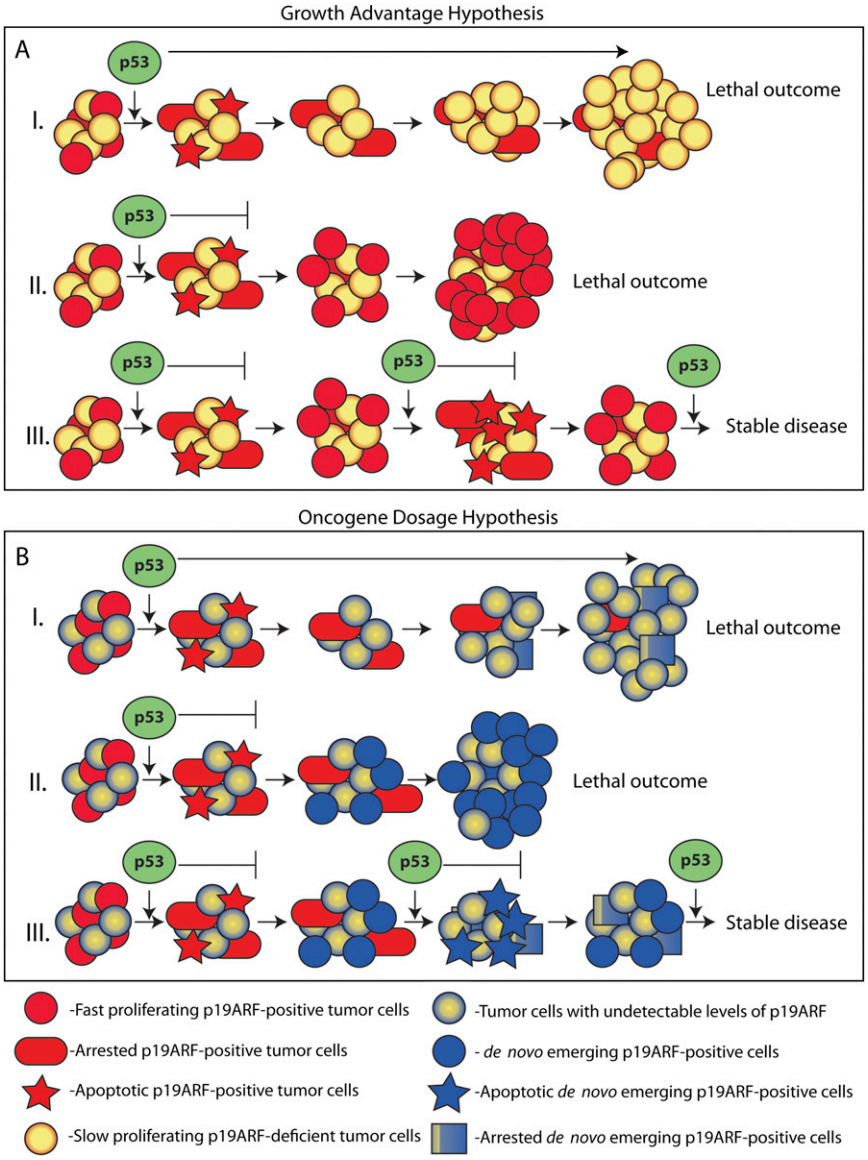

Fig. S8. Possible mechanisms behind the therapeutic advantage of intermittent versus sustained restoration of p53. (*A*) A schematic representation of the growth advantage hypothesis that $p19^{ARF}$-positive tumor cells have higher proliferating capacity than tumor cells lacking the $p19^{ARF}$ expression. (I) In the presence of sustained activation of p53, $p19^{ARF}$-negative tumor cells continue to proliferate and generate tumors resistant to subsequent p53 restoration. (II) Upon single transient p53 restoration, the majority of $p19^{ARF}$-positive cells undergo apoptosis and reversible growth arrest. The surviving $p19^{ARF}$-positive cells are capable of regenerating the tumor mass faster than their $p19^{ARF}$-negative counterparts. (III) Further intermittent restoration of p53 in mostly $p19^{ARF}$-positive tumors results in p53-induced apoptosis and promotes survival of the tumor-bearing animals. (*B*) A schematic representation of the oncogene dosage hypothesis that the tumor mass consists of cells expressing high and low levels of $p19^{ARF}$ depending on the level of rat sarcoma (Ras) oncogene activation. The proliferation status of the cells expressing low levels of $p19^{ARF}$ is independent of p53 functionality as described by Murphy et al. (1). (I) Upon sustained restoration of p53, the cells expressing high levels of $p19^{ARF}$ undergo apoptosis or growth arrest in response to functional p53, whereas cells expressing low levels of $p19^{ARF}$ continue to proliferate in a manner independent of p53 status. (II) Transient activation of p53 results in the elimination of the preexisting cells expressing high levels of $p19^{ARF}$. However, some of the preexisting $p19^{ARF}$-negative cells might be converted to cells expressing high levels of $p19^{ARF}$ because of an increase in Ras signaling or the accumulation of additional mutations. (III) The converted cells become sensitive to p53 restoration and can be targeted by additional rounds of p53 treatment.

1. Murphy DJ, et al. (2008) Distinct thresholds govern Myc's biological output in vivo. *Cancer Cell* 14(6):447–457.

Movie S1. Live images of a symptomatic *GFAP-HRas^{V12};p53$^{KI/KI}$* animal (ID#33782) taken 10 min before exposure to TAM.

Movie S1

Movie S2. Live images of a symptomatic *GFAP-HRas^{V12};p53$^{KI/KI}$* animal (ID#33782) taken 7 d after exposure to TAM.

Movie S2